Path Integral Monte Carlo for Fermions

Summer school "QMC Theory and Fundamentals"

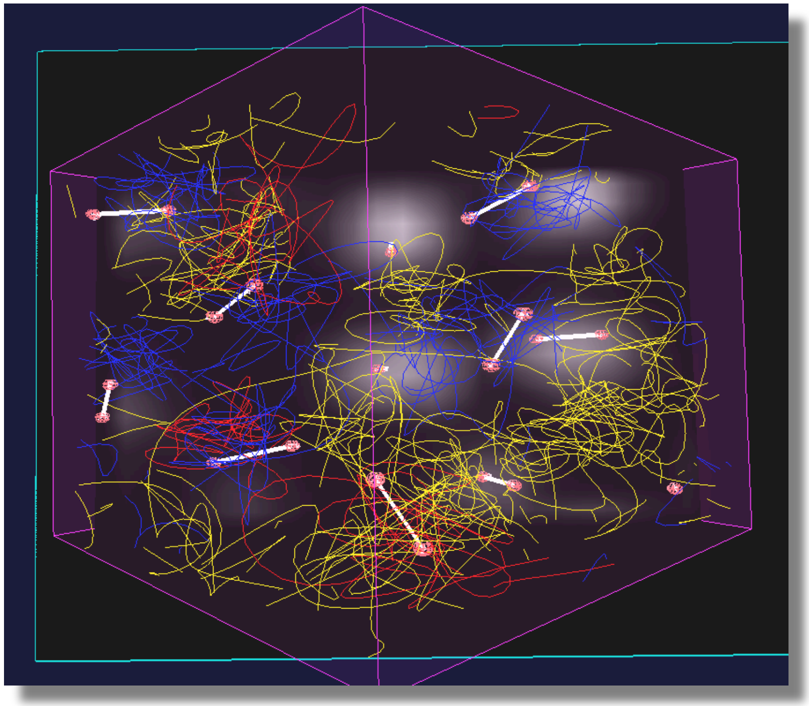

Burkhard Militzer

University of California, Berkeley

militzer@berkeley.edu

http://militzer.berkeley.edu

PIMC is the best simulation method for fermions in moderately and highly excited states:

Hydrogen plasma in the sun, some giant planets and for simulation of fusion processes

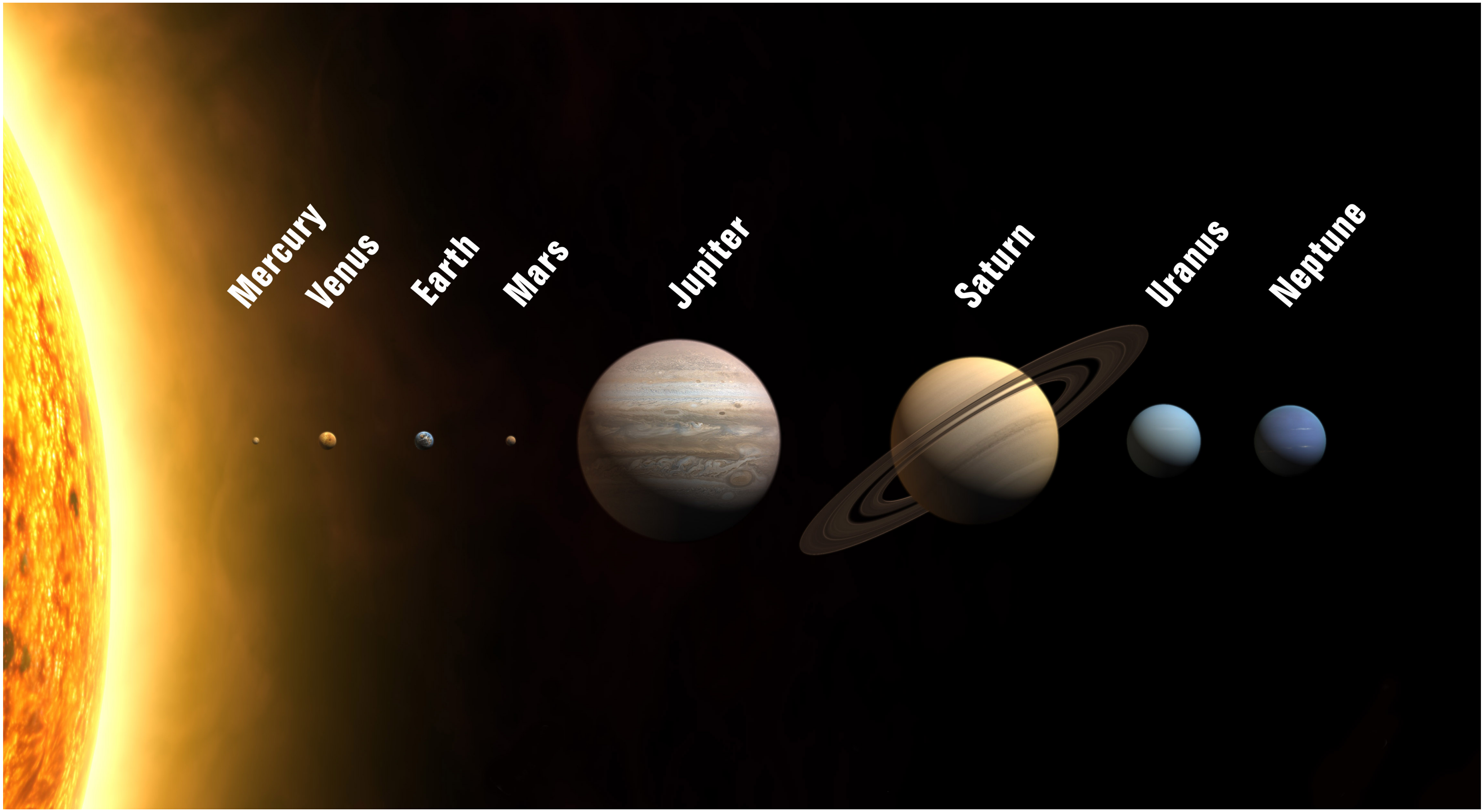

NASA’s Kepler Mission

- Determine the frequency of Earth-size and larger planets in the habitable zone of sun-like stars
- Determine the size and orbital period distributions of planets

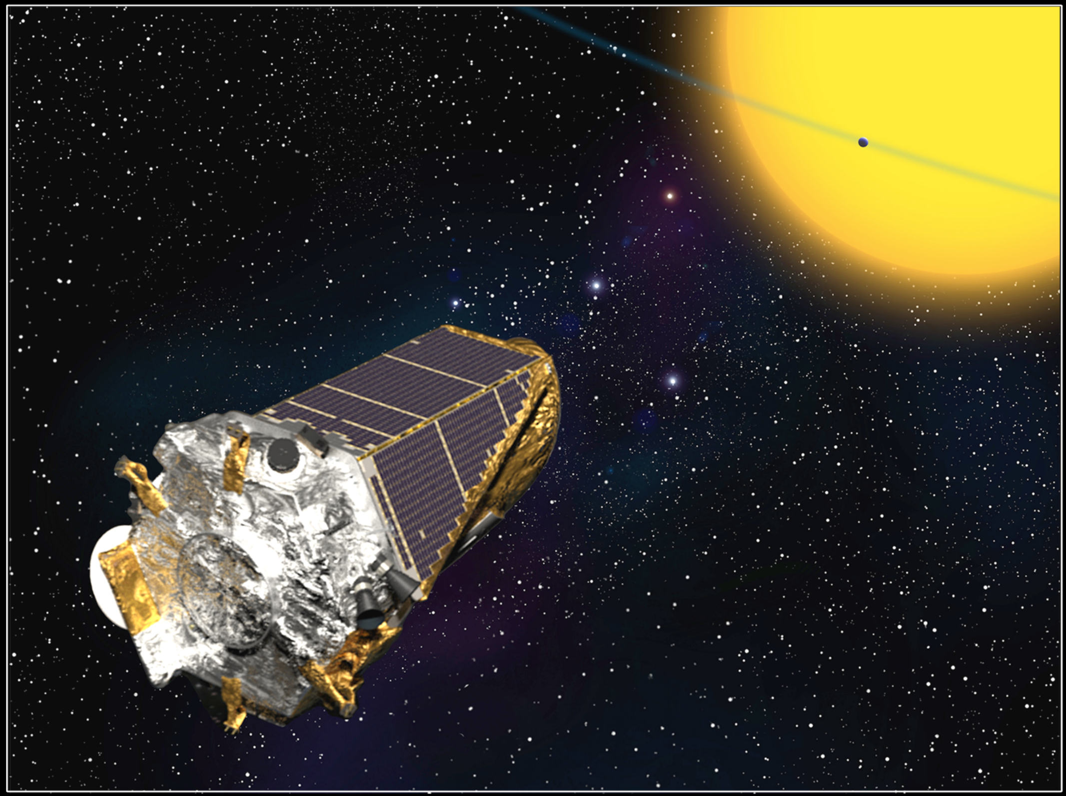

Pre-Kepler Transiting Planets - 2009

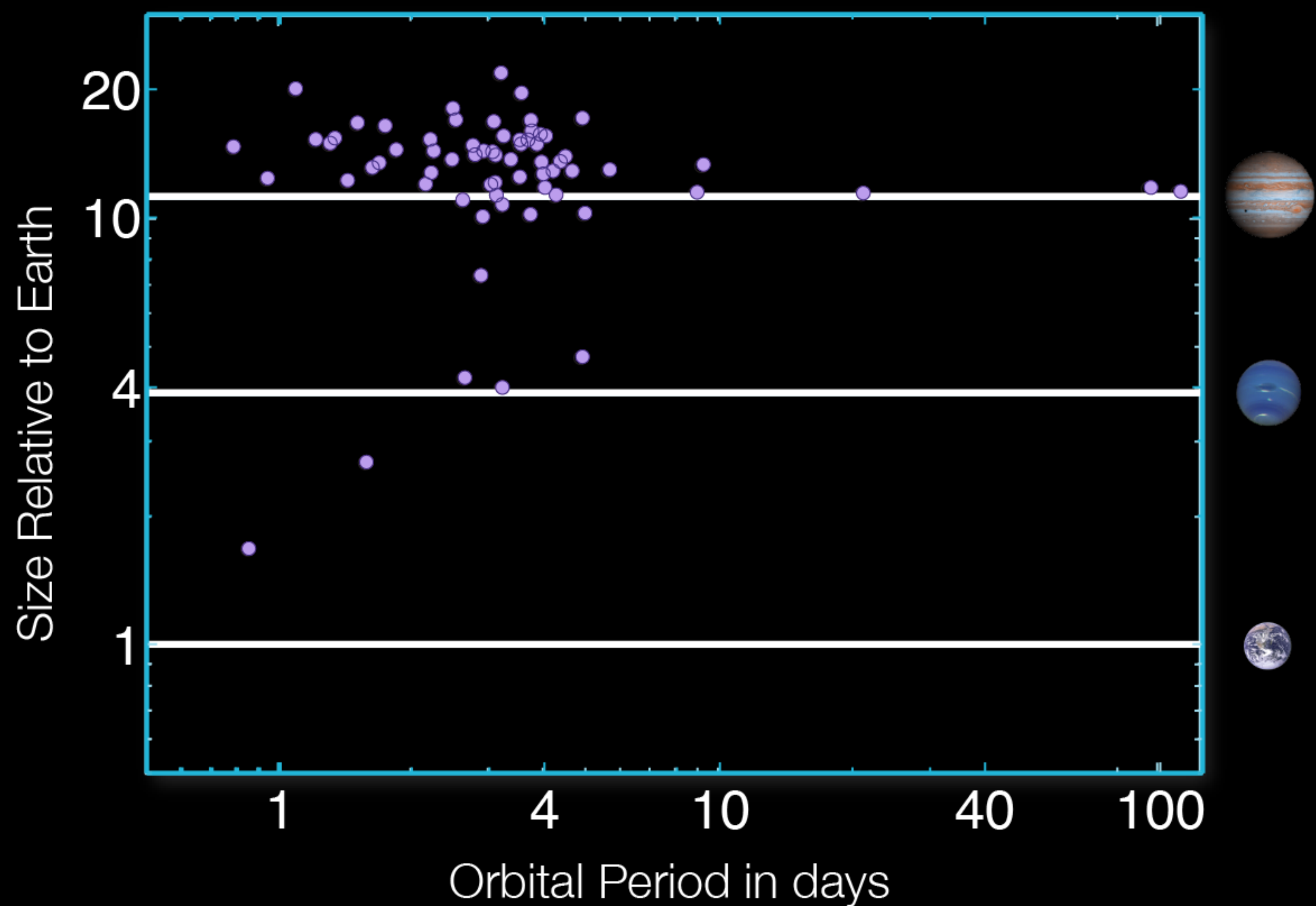

Kepler Candidates as of February 1, 2011

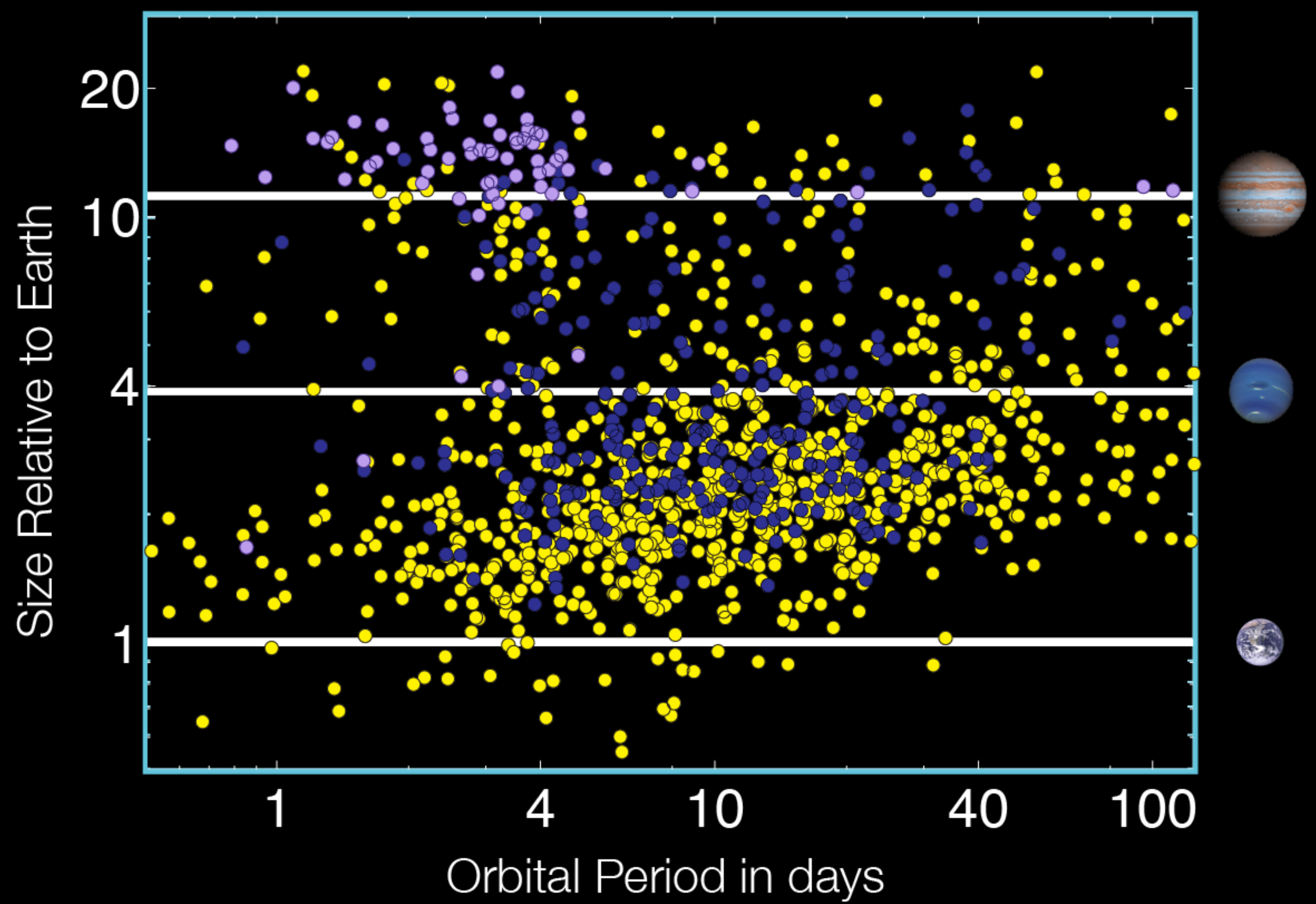

Ab initio Simulations to Characterize of the Interiors of Giant Planets

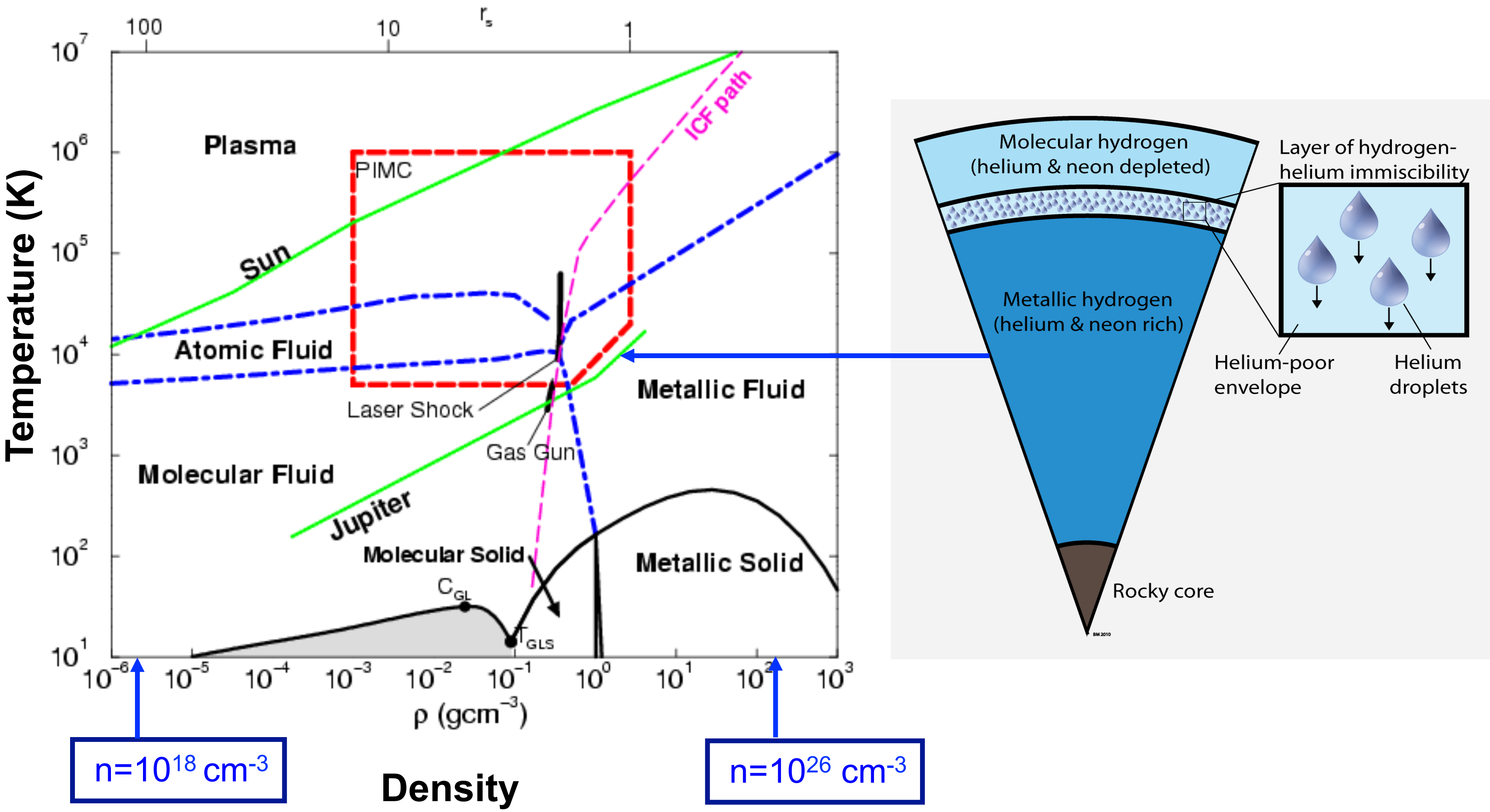

Use analytical (chemical) models at low density and very high temperature

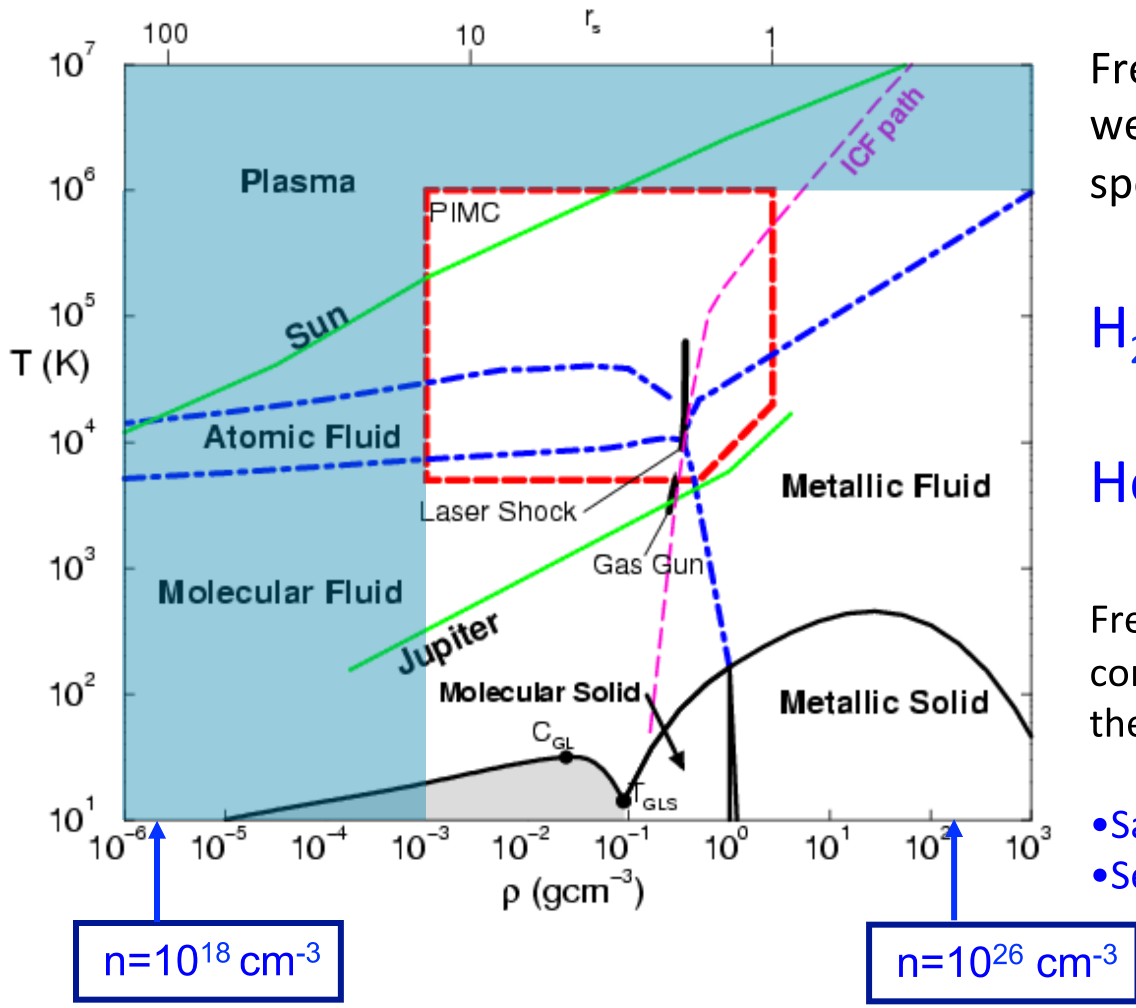

Free energy model to describe weakly interacting chemical species:

H_2, H, H^+, e^-

He, He^+, He^{++}, e^-

Free energy is constructed but it contains free parameters to describe the interaction.

- Saumon and Chabrier model (H+He)
- Sesame data base (many substances)

Density functional molecular dynamics (DFT-MD)
Couple Ion-Electron Monte Carlo (CEIMC) for lower temp.

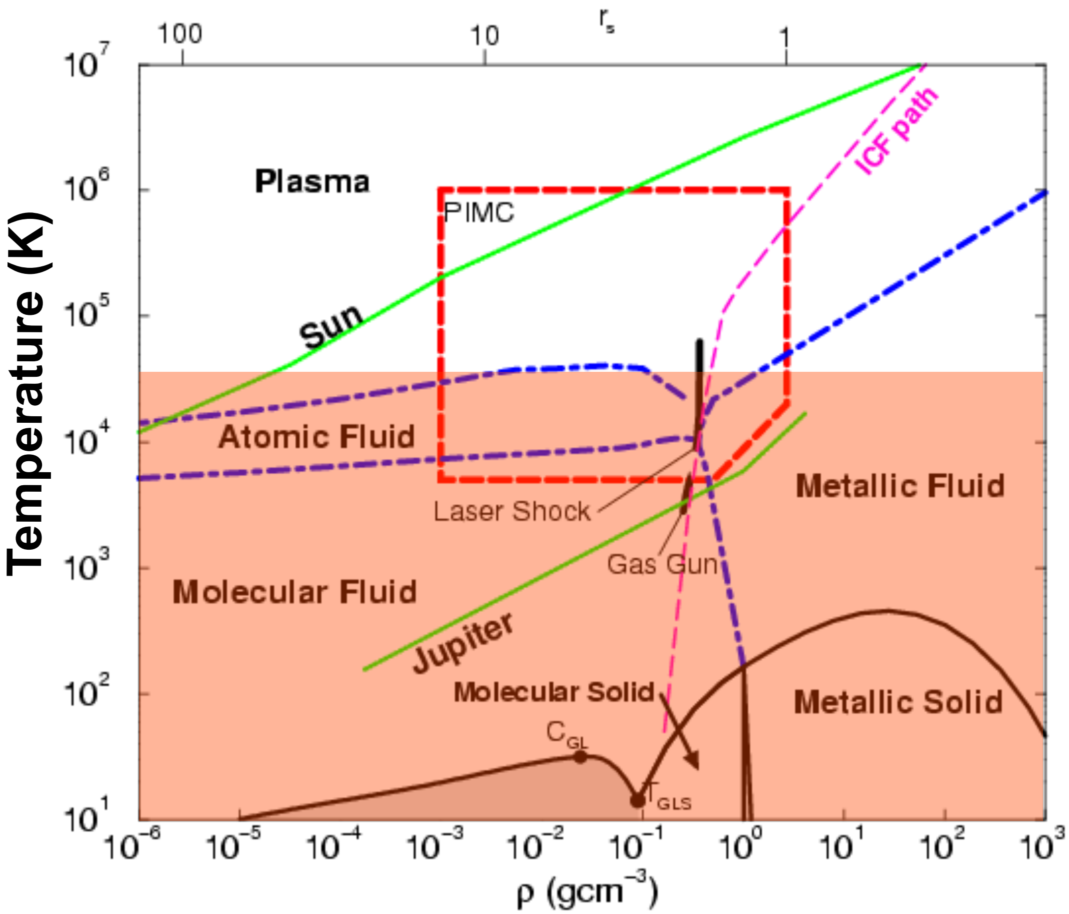

Density

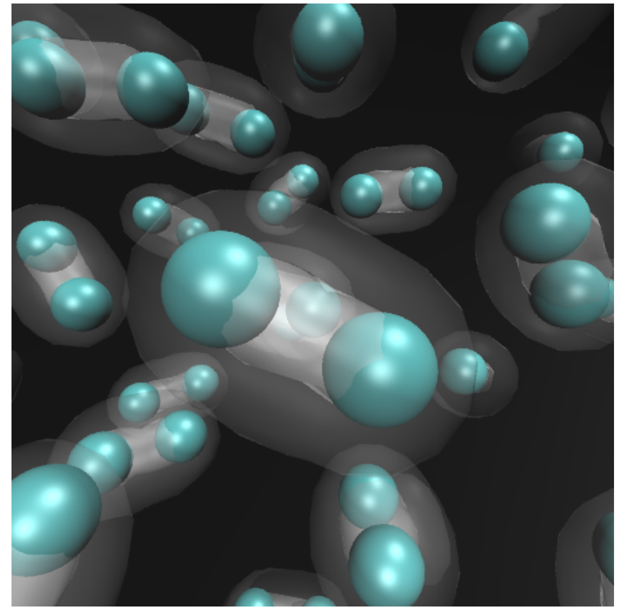

Born-Oppenheimer approx.
MD with classical nuclei:

F = m a

Forces derived DFT with electrons in the instantaneous ground state.

Path integral Monte Carlo for higher temperatures where electronic excitations are present

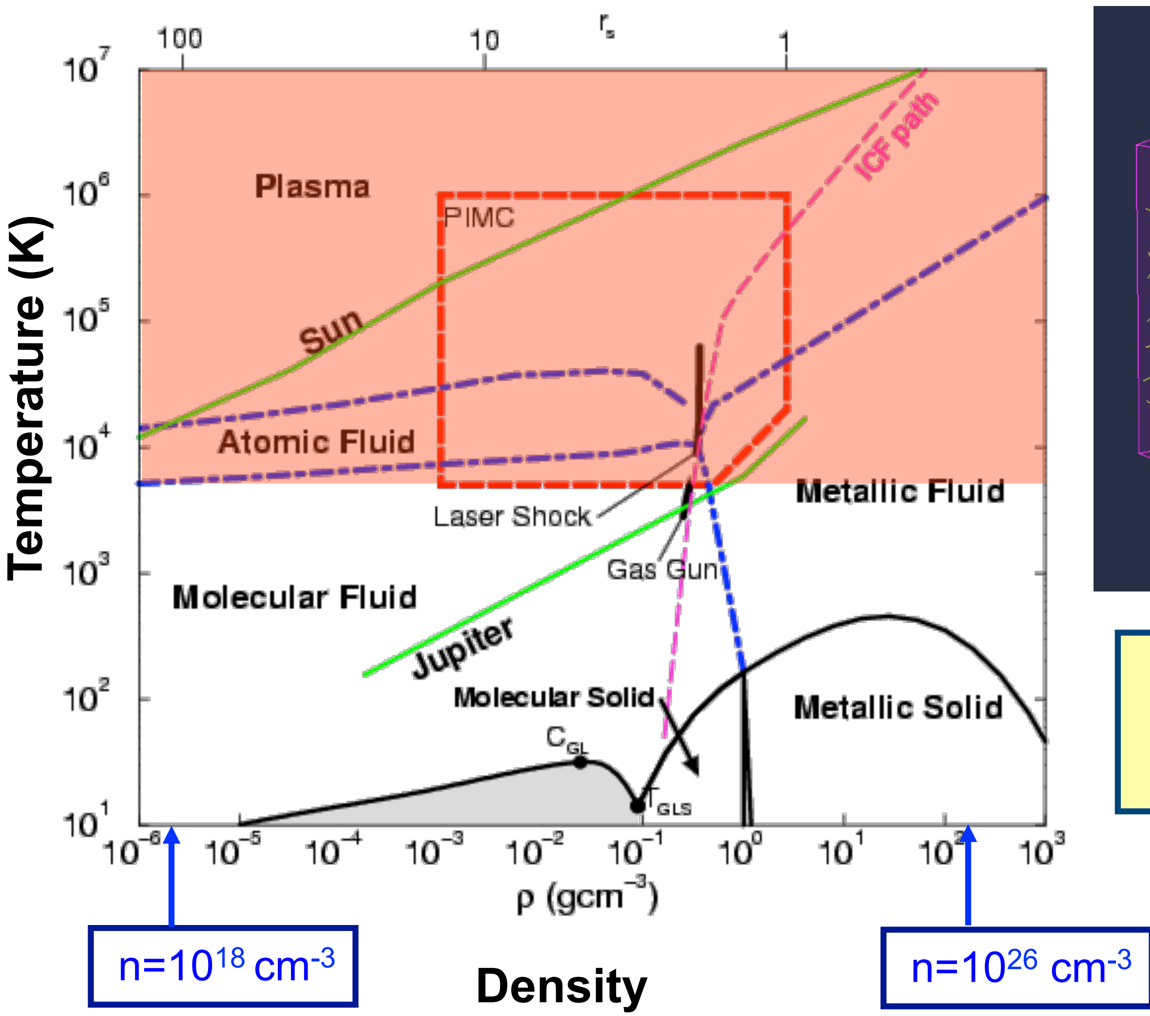

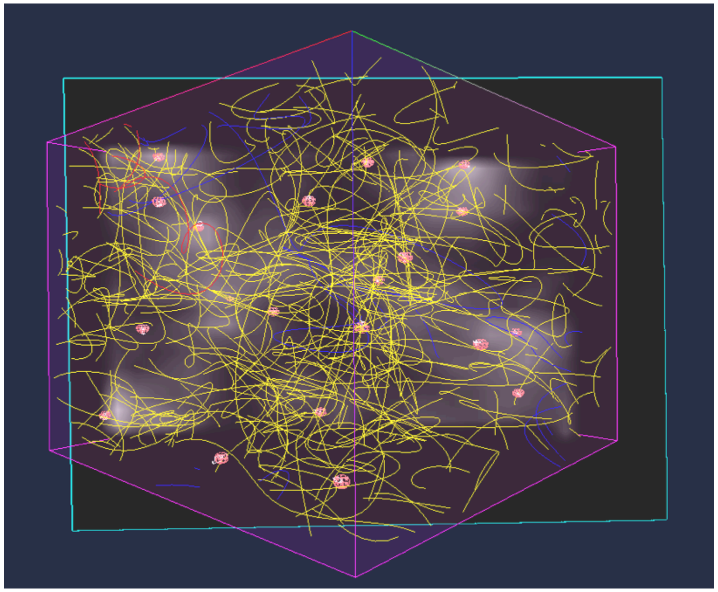

PIMC applicable at:
T>5000K

I. Fermion PIMC with and without nodes

Fermions lead to Permutations that Carry a Negative Sign

Fermionic density matrix:
Sum over all antisymmetric eigenstates.

$$\rho_F(R,R',\beta) = \sum_i e^{-\beta E_i} \; \Psi_{AS}^{[i]*}(R) \; \Psi_{AS}^{[i]}(R')$$

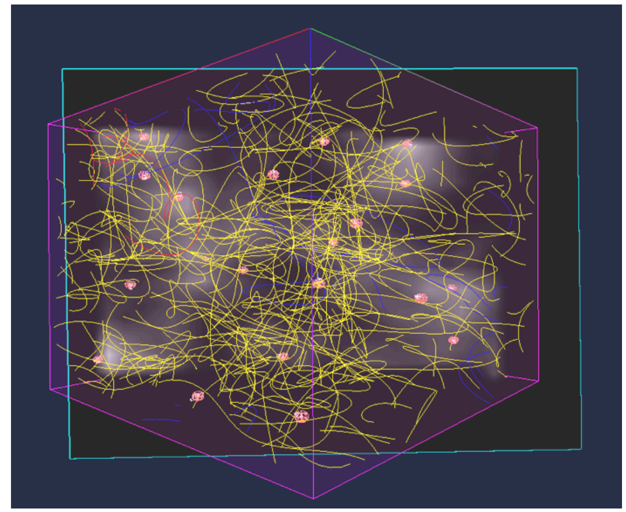

Project out the antisymmetric states:

$$\rho_F(R,R',\beta) = \sum_P (-1)^P \; \rho_D(R,PR',\beta)$$

$$\langle R \mid \hat{\rho}_{F/B} \mid R' \rangle = \sum_P (\pm 1)^P \int dR_1 \ldots \int dR_{M-1} \langle R \mid e^{-\tau \hat{H}} \mid R_1 \rangle \ldots \langle R_{M-1} \mid e^{-\tau \hat{H}} \mid PR' \rangle$$

D:

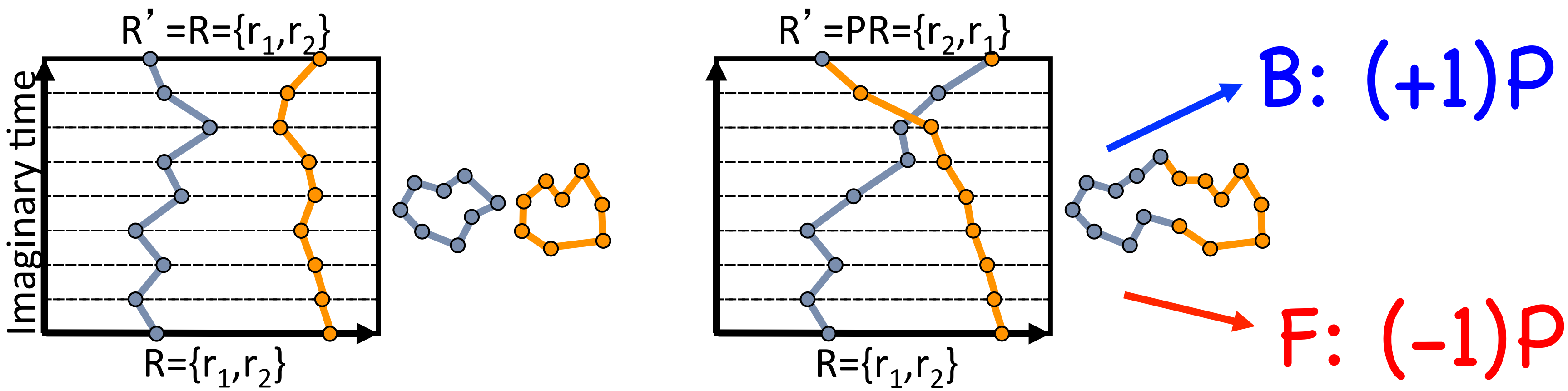

“Direct” Fermion Path Integrals

The fermion sign problem poses a major challenge.

$$\langle R|\hat{\rho}_F|R'\rangle = \sum_P (-1)^P \int dR_1 \ldots \int dR_{M-1} \langle R|e^{-\tau\hat{\mathrm{H}}}|R_1\rangle \ldots \langle R_{M-1}|e^{-\tau\hat{\mathrm{H}}}|PR'\rangle$$

How do evaluate an integral with negative and positive contributions with MC?
→ Let us try the “direct” fermion method first:

- Sample all path with the bosonic action including permutations, P
- Add a weight factor of **$(-1)^P$** when the observables are computed.

$$\langle O\rangle_F = \frac{\langle \sigma(P) O(R)\rangle_B}{\langle \sigma(P)\rangle_B} \qquad \sigma(P) = (-1)^{\mathrm{P}}$$

- This is exact, but positive and negative contributions cancel to a large extent
  → Fermion sign problem
- The efficiency of the algorithm scale like (Ceperley 1995)

$$\xi = \left[\frac{M_+ - M_-}{M_+ + M_-}\right]^2 = \left[\frac{Z_F}{Z_B}\right]^2 = \exp[-2\beta(F_F - F_B)] = \exp[-2\beta N(\mu_F - \mu_B)]$$

Fixed-Node Method for Fermion PIMC

- Get rid of negative walks by canceling them with some of the positive walks. We can do this if we know where the density matrix changes sign. Restrict walks to those that stay on the same side of the node.
- Fixed-node identity. Gives exact solution if we know the places where the density matrix changes sign: the nodes.

$$\rho_F(R_\beta, R_*; \beta) = \frac{1}{N!} \sum_P (-1)^P \int_{\rho_F(R_t, R_*; t) > 0} dR_t e^{-S(R(t))} \text{ with } R_0 = \mathrm{P}R_*$$

- Classical correspondence exists!!
- Problem: fermion density matrix appears on both sides of the equation. We need nodes to find the density matrix.

Proof of the fixed node method for path integrals

1. The density matrix satisfies the Bloch equation with initial conditions.

$$\frac{\partial \rho(R,t)}{\partial t} = \hat{H}\rho(R,t) = \lambda \nabla^2 \rho(R,t) - V(R)\rho(R,t) \qquad \rho(R,0) = \frac{1}{N!}\sum_P (-1)^P \delta(R - PR_0)$$

2. One can use more general boundary conditions, not only initial conditions, because solution at the interior is uniquely determined by the exterior-just like the equivalent electrostatic problem.
3. Suppose someone told us the surfaces where the density matrix vanishes (the nodes). Use them as boundary conditions.
4. Putting an infinite repulsive potential at the barrier will enforce the boundary condition.
5. Returning to PI' s, any walk trying to cross the nodes will be killed.
6. This means that we just restrict path integrals to stay in one region.

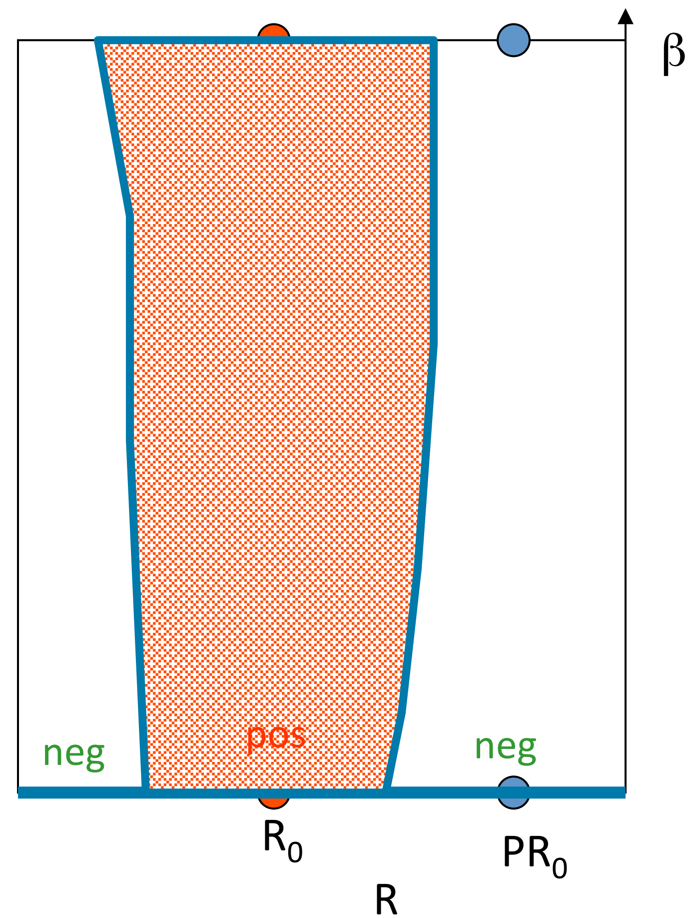

Slide - David Ceperley

What nodes shall we used in PIMC?

- To get around the sign problem, why not just use the fixed-node method from T=0 calculation?
- What nodes? The ground state nodes are not necessarily the correct ones at T>>0.
- The nodes of the density matrix have an imaginary time dependence: $\rho_F\left(R,R_0;t\right)=0 \quad \text{with} \quad R_0,t \quad \text{fixed.}$

High temperature

Low temperature

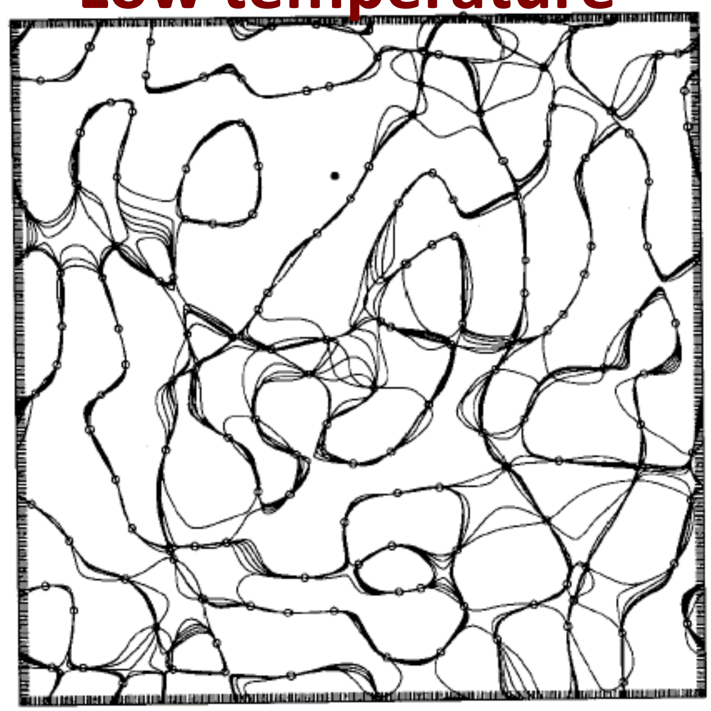

Slide - David Ceperley

Simplest type of nodes: Free particles nodes they are exact at high temperature

Construct a **fermionic trial density matrix** in form of a Slater determinant of single-particle density matrices:

$$\rho_T(R,R',\beta) = \begin{vmatrix} \rho_0(r_1,r_1',\beta) & \cdots & \rho_0(r_1,r_N',\beta) \\ \vdots & \ddots & \vdots \\ \rho_0(r_N,r_1',\beta) & \cdots & \rho_0(r_N,r_N',\beta) \end{vmatrix}$$

Free particle density matrix:

$$\rho_0(r,r',\beta) = \frac{1}{V}\int d^3k\ e^{-\beta\lambda k^2} e^{-ikr}\ e^{+ikr'}$$

$$\rho_0(r,r',\beta) = (4\pi\lambda\beta)^{-D/2}\quad \exp\left[-\frac{(r-r')^2}{4\lambda\beta}\right]$$

Enforce the following nodal condition for all time slices along the paths:

$$\rho_T\left[R(t),R(0),t\right] > 0$$

This 3N-dimensional conditions eliminates all negative and some positive contribution to the path [Ceperley et al. 1995]
⇒"Solves" the fermion sign problem.

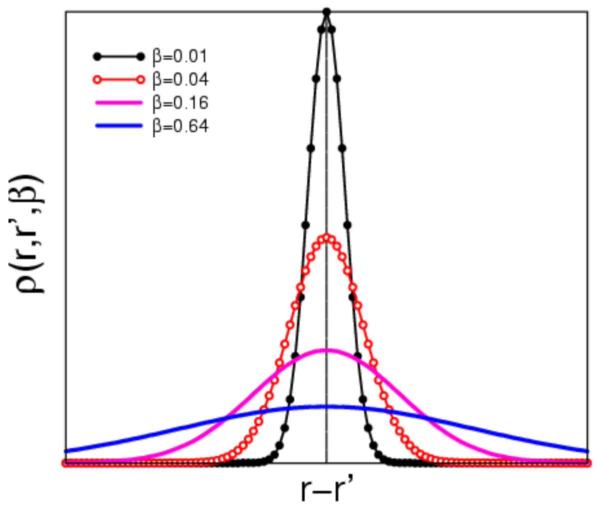

$$\lambda = \frac{\hbar^2}{2m}$$

$$\beta = \frac{1}{k_b T}$$

Nodal action

- Principal rule: simply reject paths if they cross a node.
- Will lead to an error proportional to $\sqrt{\lambda\tau} / r_{nn}$
- Improved nodal action: solve for a particle next to a planar node. Use method familiar from electrostatics, the method of images:

$$\rho(r',r;t) = e^{-\frac{(r-r')^2}{4\lambda\tau}} - e^{-\frac{(r-r^*)^2}{4\lambda\tau}} \qquad r^* = -r'$$

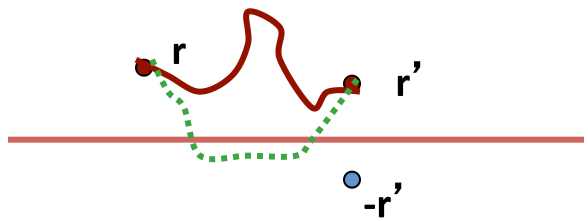

$$\delta S(r',r;t) = -\ln\left(1 - \mathrm{e}^{-\frac{dd'}{\lambda\tau}}\right) \qquad \mathrm{d{=}distance\ to\ node} \approx \left|\nabla \ln\left(\rho\left(R,R';\tau\right)\right)\right|^{-1}$$

- Determine nodal distance using "Newton estimate."
- As paths approach within a thermal wavelength of the node, we get a repulsion, to account for the probability that a path could have crossed and recrossed within τ.

II. Better nodes: Variational Density Matrix

Derivation of a Variational Density Matrix

(see Militzer, Pollock, Phys. Rev. E 61 (2000) 3470)

Bloch equation: $$-\frac{\partial \rho}{\partial \beta} = \mathcal{H}\rho$$

Ansatz for density matrix

$$\rho(\mathcal{R},\mathcal{R}';\beta) = \rho(\mathcal{R},q_1,\ldots,q_m) \qquad q_k = q_k(\mathcal{R}',\beta)$$

Variational principle: $\delta I = 0$

$$I\left(\frac{\partial \rho}{\partial \beta}\right) = \int d\beta \int d\mathcal{R} \left(\frac{\partial \rho}{\partial \beta} + \mathcal{H}\rho\right)^2$$

$\Rightarrow$ ordinary differential equations for q_k in imaginary time

Slater determinant: $\rho(\mathcal{R},\mathcal{R}';\beta) = \left\|\rho^{[1]}(\mathbf{r}_i,\mathbf{r}'_j;\beta)\right\|_{ij}$

Gaussian Ansatz:

$$\rho^{[1]}(\mathbf{r},\mathbf{r}',\beta) = (\pi w)^{-3/2} \exp\left\{-\frac{1}{w}(\mathbf{r}-\mathbf{m})^2 + d\right\}$$

Variational parameters:
- $\mathbf{m}$ ... mean position $(= r')$
- w ... squared width $(=4\lambda\beta)$
- d ... amplitude $(=0)$

Derivation of a Variational Density Matrix

(see Militzer, Pollock, Phys. Rev. E 61 (2000) 3470)

Gaussian Ansatz:

$$\rho^{[1]}(\mathbf{r},\mathbf{r}',\beta) = (\pi w)^{-3/2} \exp\left\{-\frac{1}{w}(\mathbf{r}-\mathbf{m})^2 + d\right\}$$

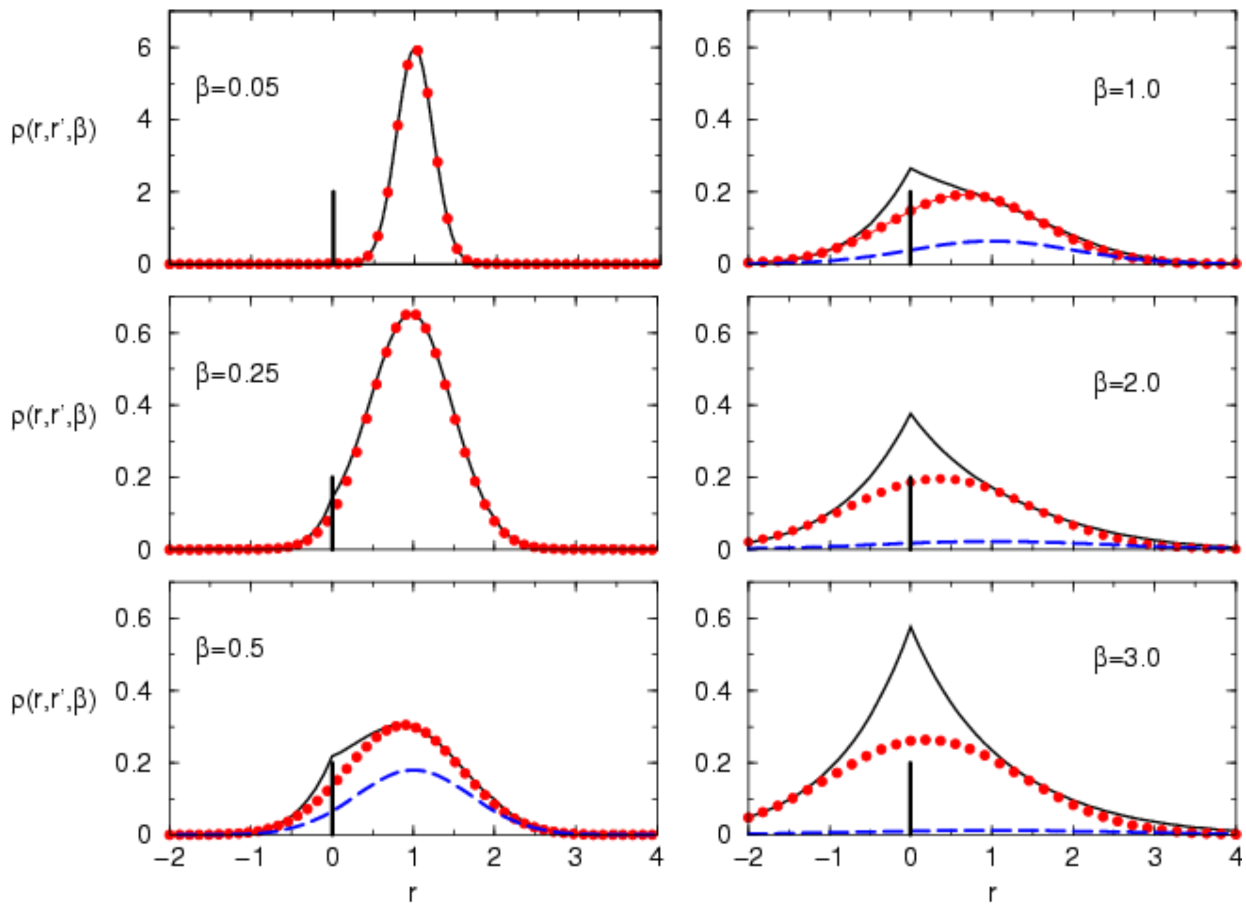

Comparison: T=0 and T>0 Fermion Methods

Analogy to Ground State Methods

$T = 0$	$T > 0$
$\Psi_{GS}(\mathbf{R})$	$\rho(\mathbf{R},\mathbf{R}';\beta) = \Sigma_s\, e^{-\beta E_s}\Psi_s(\mathbf{R})\boldsymbol{\Psi}_\mathbf{s}(\mathbf{R}')$
$E \leq <\Psi\|H\|\Psi> / <\Psi\|\Psi>$	$F \leq \mathrm{Tr}[\tilde{\rho} H] + kT\ \mathrm{Tr}[\tilde{\rho}\ln\tilde{\rho}] \quad \tilde{\rho} = \rho/\mathrm{Tr}[\rho]$

1. Effective Single Particle Level

$$\Psi_{KS}(\mathbf{R}) = \begin{vmatrix} \Phi_1(r_1) & \dots & \Phi_N(r_1) \\ \dots & \dots & \dots \\ \Phi_1(r_N) & \dots & \Phi_N(r_N) \end{vmatrix}$$

$$\rho(\mathbf{R},\mathbf{R}';\beta) = \begin{vmatrix} \rho^{[1]}(r_1,r_1';\beta) & \dots & \rho^{[1]}(r_N,r_1';\beta) \\ \dots & \dots & \dots \\ \rho^{[1]}(r_1,r_N';\beta) & \dots & \rho^{[1]}(r_N,r_N';\beta) \end{vmatrix}$$

LDA: $\epsilon_s\Phi_s = -\frac{\nabla^2}{2}\Phi_s + V_{eff}\Phi_s$

Variational solution of many-body Bloch Equation

2. Correlations beyond LDA or Mean Field

Jastrow	Finite Temperature Jastrow
$\Psi_{GS}(\mathbf{R}) = \Psi_{KS}(\mathbf{R})\,\Pi_{i,j}\,f(r_{ij})$	$\rho(\mathbf{R},\mathbf{R}';\beta) = \rho_{MF}(\mathbf{R},\mathbf{R}';\beta)\,\Pi_{i,j}\,f(r_{ij},r_{ij}';\beta)$

3. Diffusion QMC — Restricted PIMC

III. Example: Paths of two free particle

Fermionic Path Integrals
Example: 2 free particles

Distinguishable particles:

Consider path types: A + B

Bosons:

Consider path types: A + B + C

Direct fermions:

Consider path types: A + B – C

Restricted fermions:

Consider only path type: A

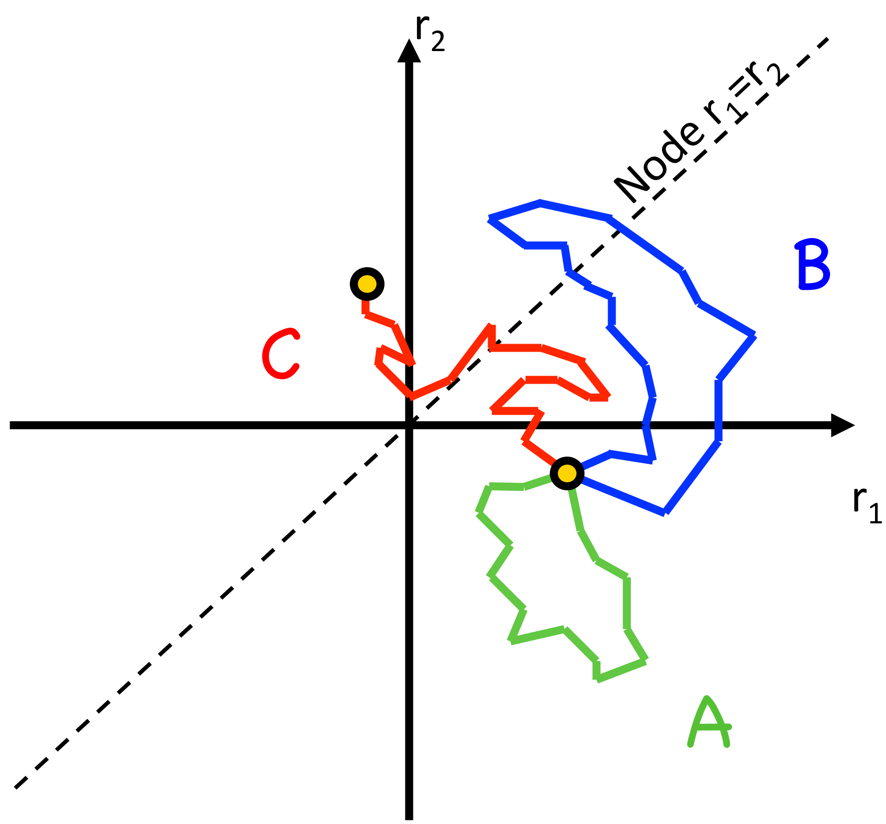

IV. Application to hot, dense hydrogen and Shock Wave Experiments

Molecular Hydrogen

Snapshot from a PIMC simulation with 32 protons and electrons

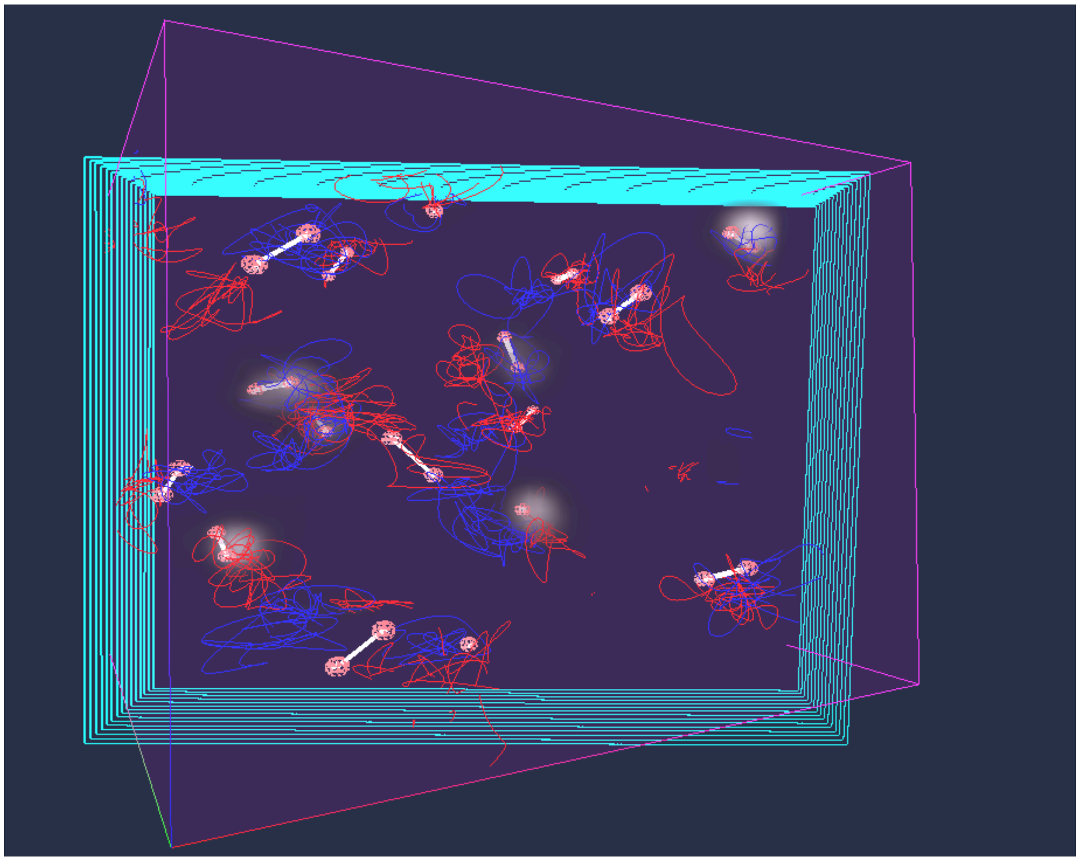

2 protons (pink spheres) and spin-up and one spin-down electron form one H_2 molecule.

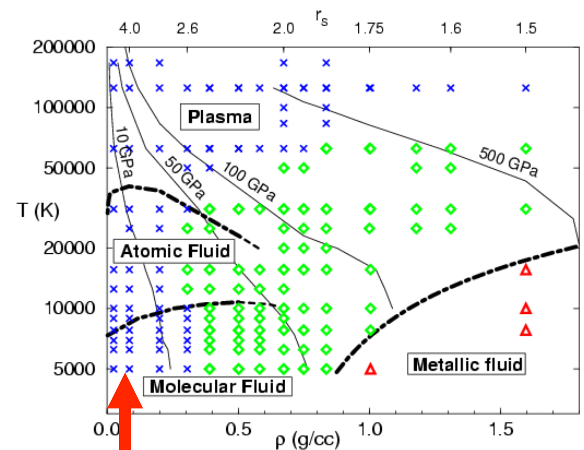

T=5000K, r_s=4

100% molecules, weakly interacting

Molecular Hydrogen

Snapshot from a PIMC simulation with 32 protons and electrons

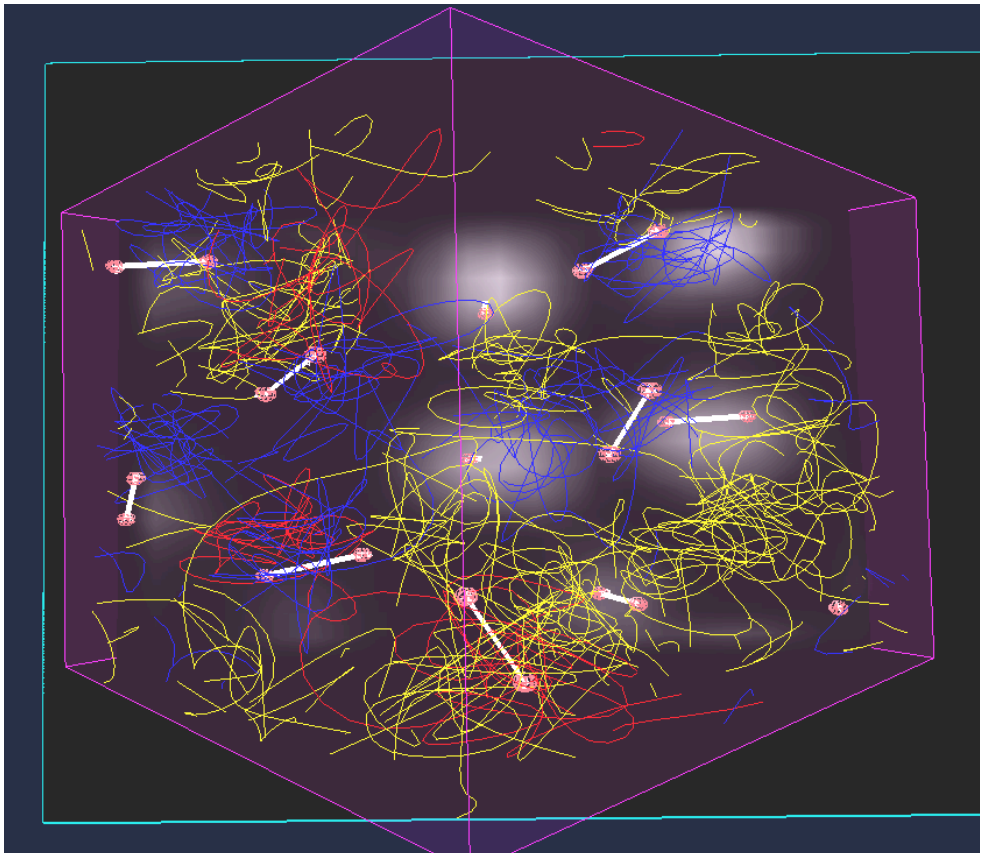

2 protons (pink spheres) and spin-up and one spin-down electron form one H_2 molecule.

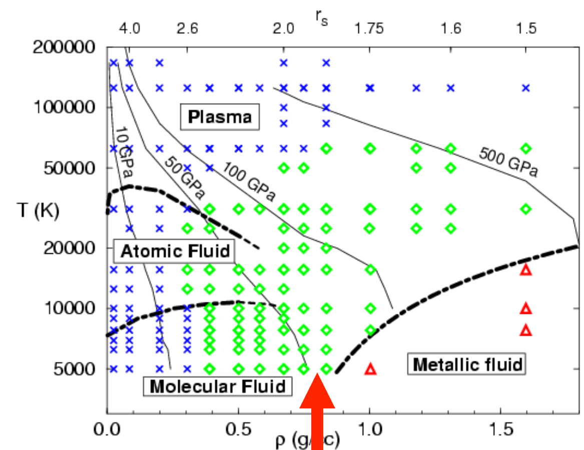

T=5000K, r_s=1.86

- strongly interacting molecules, close to pressure dissociation
- Electrons are degenerate, partially delocalized
- Electron paths are permuting

Metallic Hydrogen

Snapshot from a PIMC simulation with 32 protons and electrons

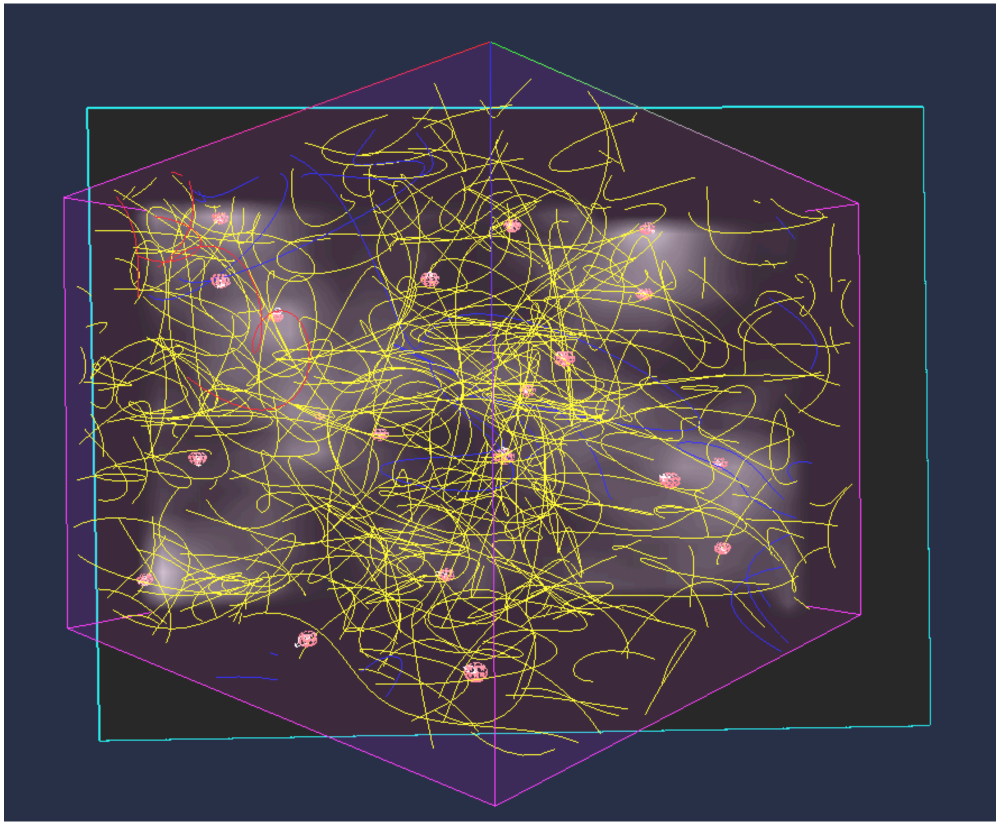

Free protons (pink spheres) and delocalized electrons.

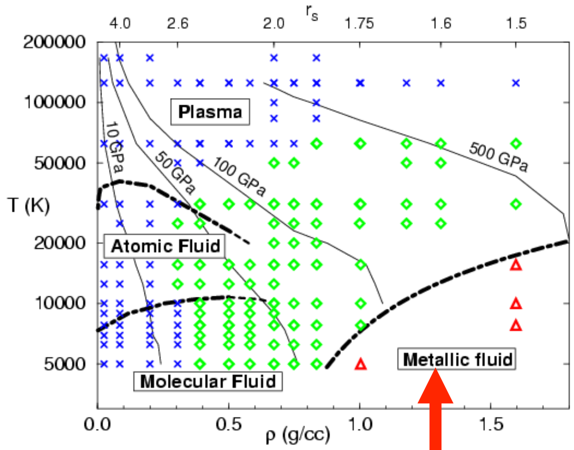

T=5000K, r_s=1.6

- Pressure dissociation, free protons
- Degenerate electron gas
- High number of permutations

Recent PIMC work provides EOS for ICF conditions (FPEOS table constructed)

Hydrogen

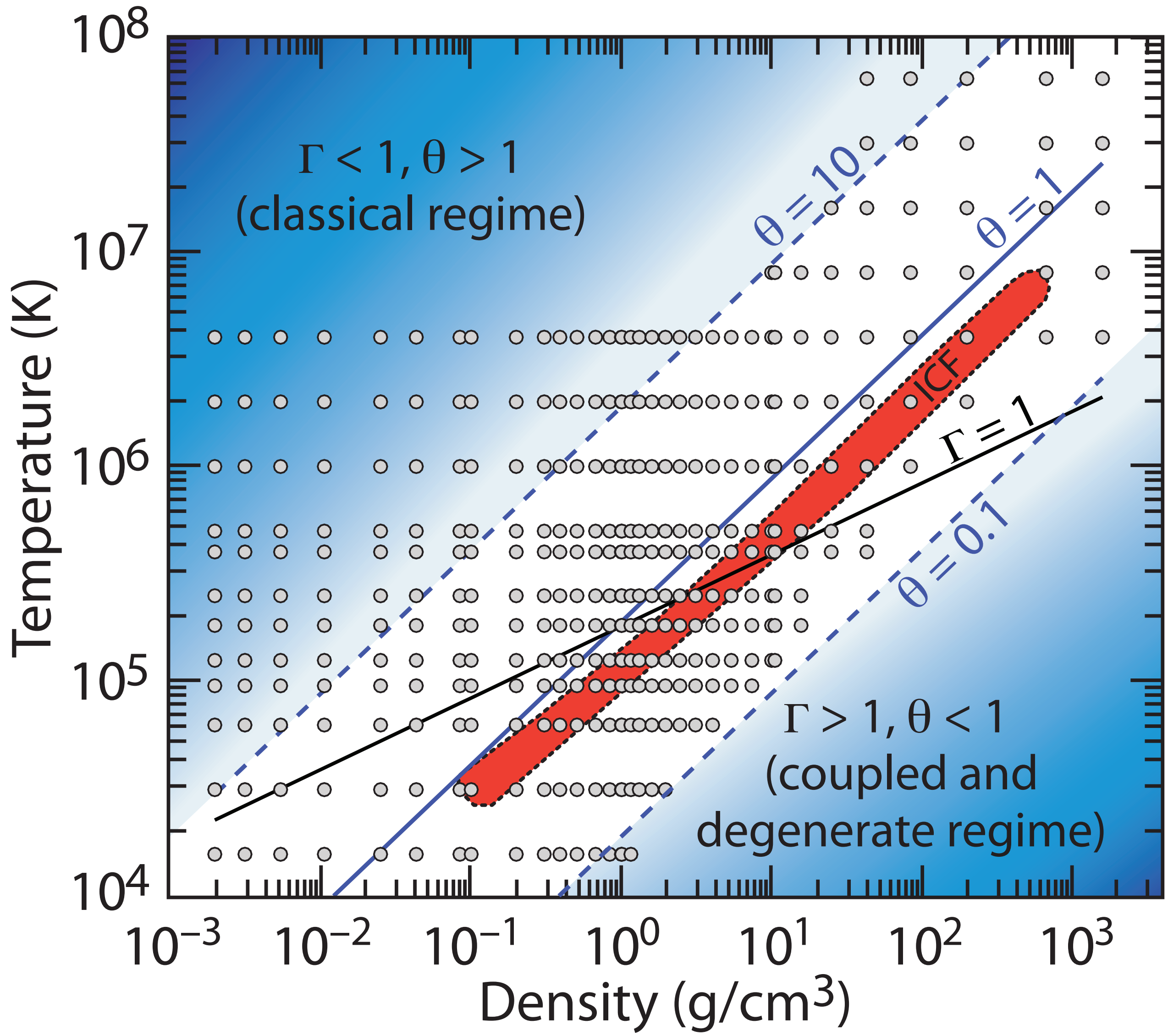

S. X. Hu, B. Militzer, V. N. Goncharov, S. Skupsky, *Phys. Rev. Lett.*, **104** (2010) 235003

Phys. Rev. B **84** (2011) 224109.

For hydrogen, PIMC and DFT-MD Simulations Predict Consistent Shock Properties

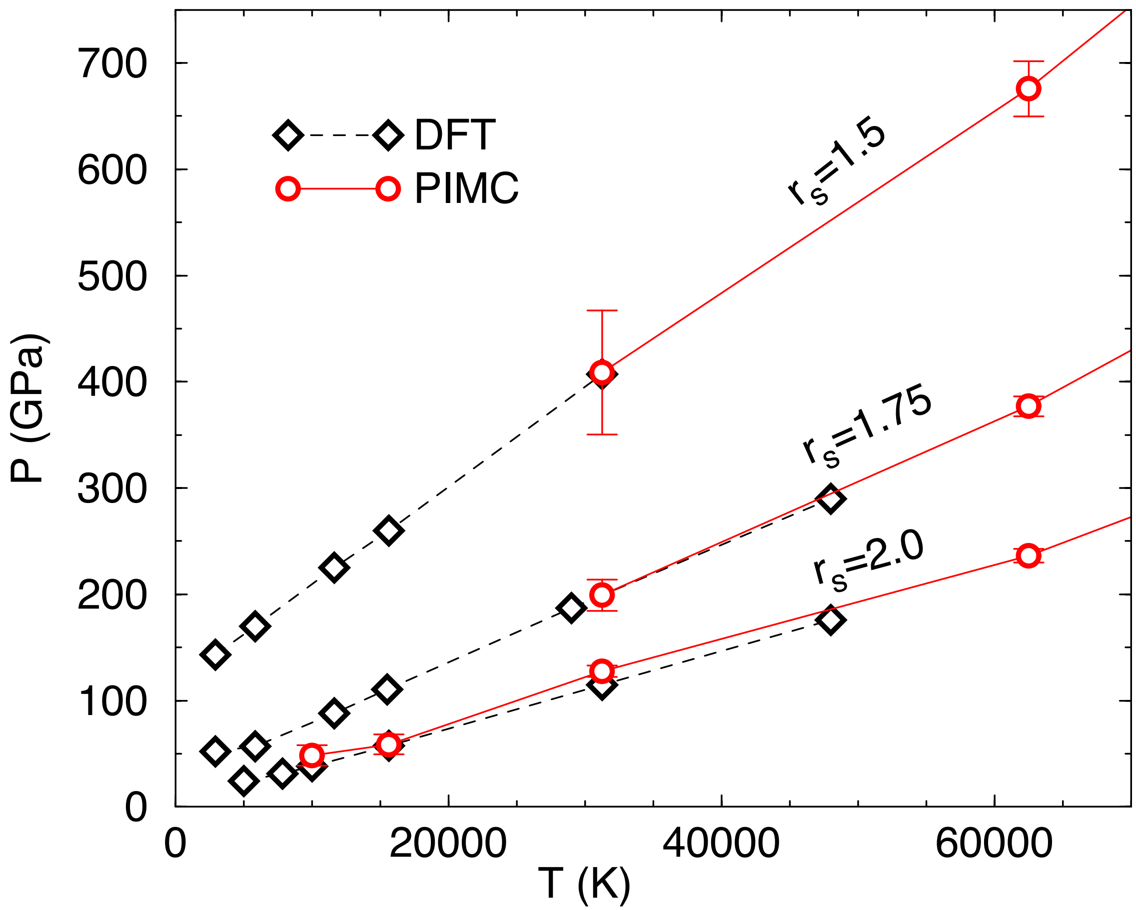

B. Militzer, D. M. Ceperley, J. D. Kress, J. D. Johnson, L. A. Collins, S. Mazevet, *Phys. Rev. Lett.* **87** (2001) 275502

Study planetary interiors in the laboratory: shock wave experiments

1) Two-stage gas gun (Livermore)
20 GPa in deuterium

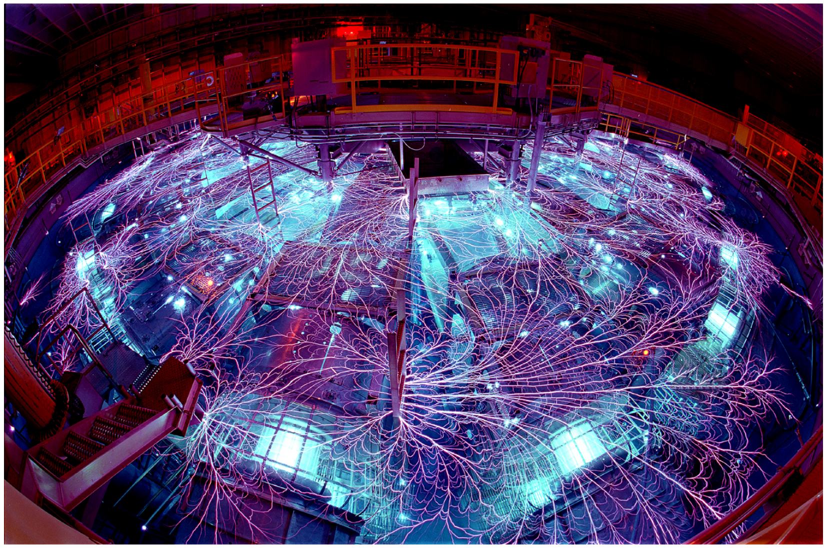

3) Z capacitor bank (Sandia) 175 GPa

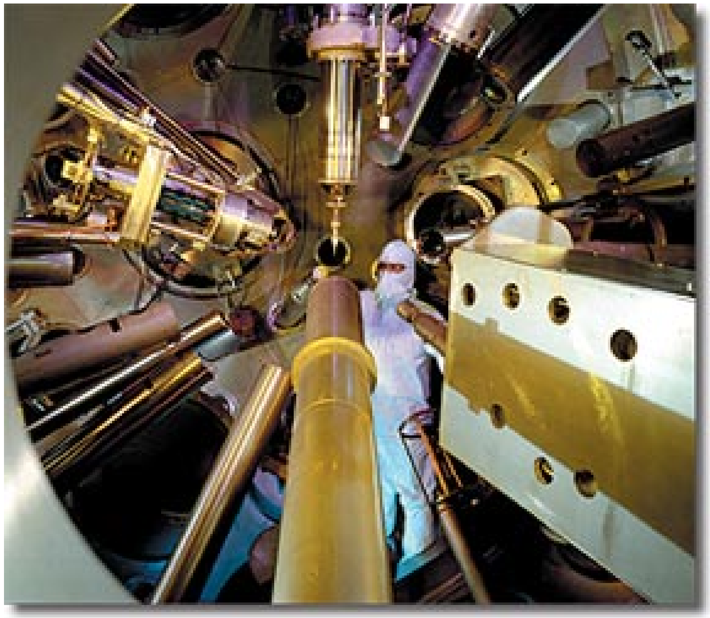

2) Nova laser (Livermore) 340 GPa

4) NIF…

Shock wave measurements determine the EOS on the Hugoniot curve

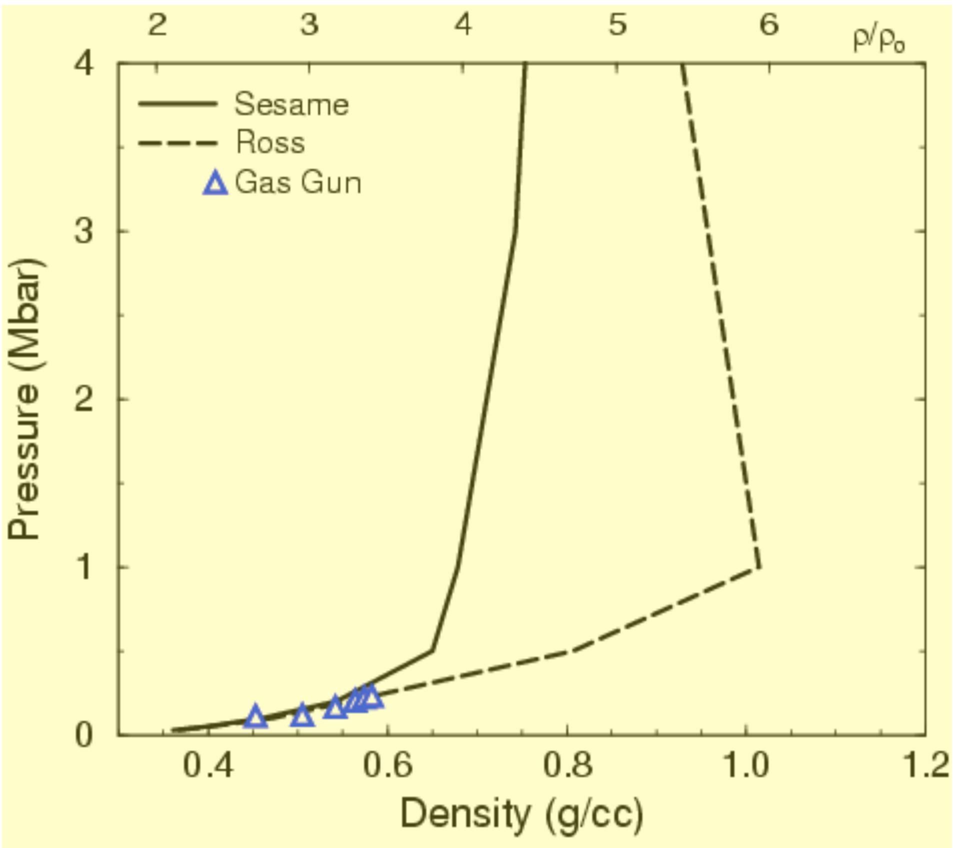

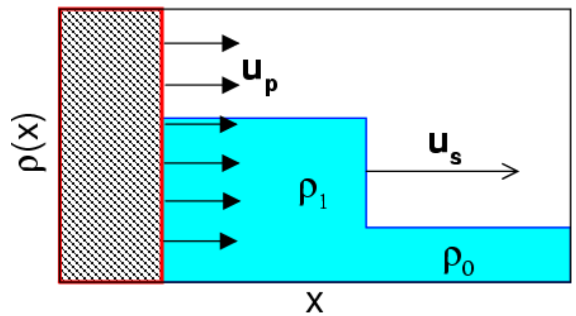

Conservation of mass, momentum and energy yields:

$$\frac{\rho}{\rho_0} = \frac{u_s}{u_s - u_p}$$

$$p - p_0 = \rho_0 u_s u_p$$

$$E - E_0 = \frac{1}{2}(V_0 - V)(P + P_0)$$

Gas gun (LLNL), Sesame model (Kerley), linear mixing model (M.Ross)

Deuterium Hugoniot

Nova laser shock wave experiments reached 3.4 Mbar

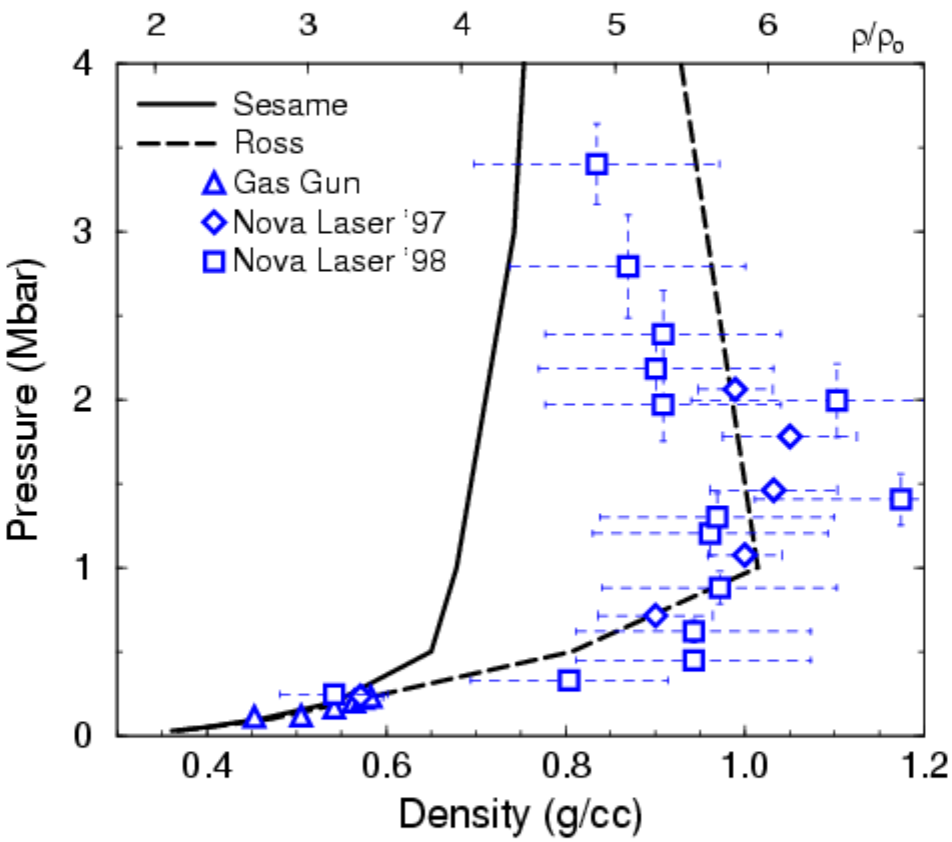

Why is the compressibility so high?

What does this imply for the dissociation of molecules?

Are electronic excitations important?

Nova laser results predict a 50% higher compressiblity.

Deuterium Hugoniot

Path integral Monte Carlo results

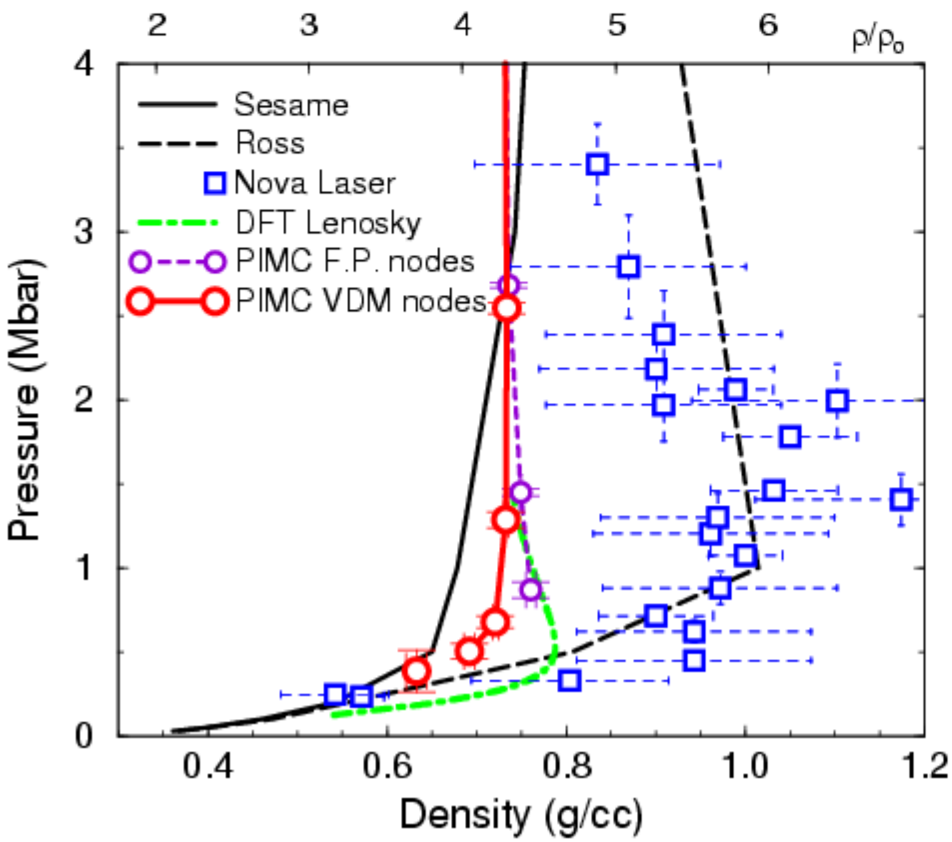

Militzer and Ceperley,
Phys. Rev. Lett. 85 (2000) 1890.
Phys. Rev. Lett. 87 (2001) 275502

- Accuracy increases with T
- Small size dependence
- Comparison of VDM and free particle nodes

Discrepancy:
$\Delta E/N = 3$ eV
$\Delta PV/N = -2$ eV

Good agreement between all *ab initio* methods.

PIMC predicts low compressibility and agrees with more recent experiments

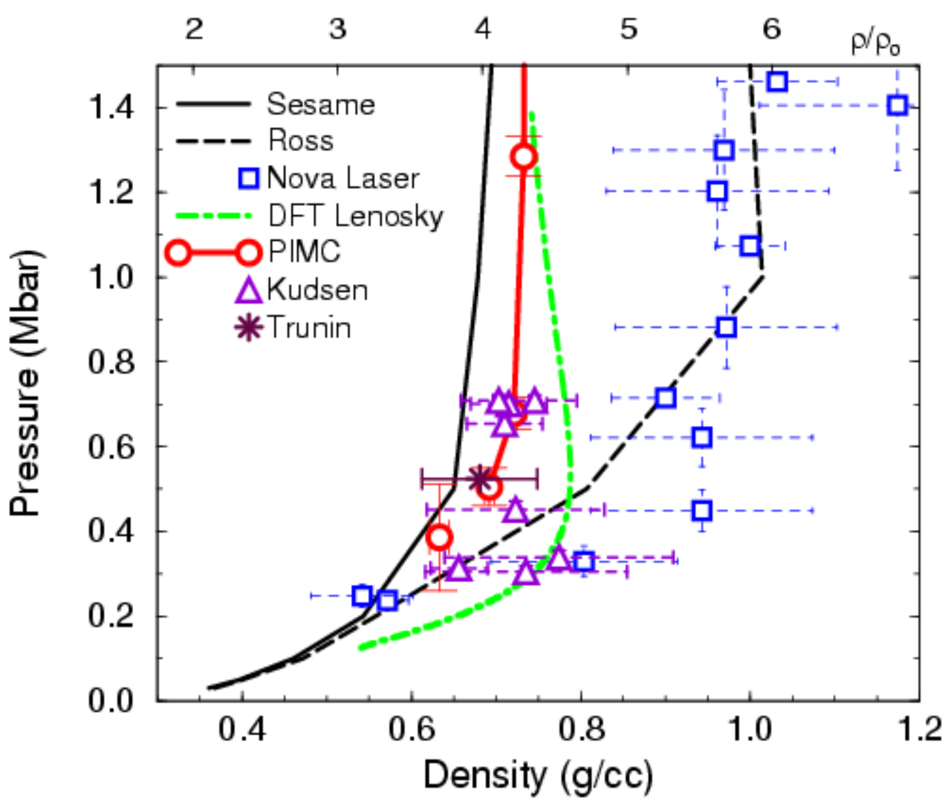

Militzer, Ceperley *et al.*
Phys. Rev. Lett. **85** (2000) 1890.
Phys. Rev. Lett. **87** (2001) 275502.

- Predict low compressibility!

Good agreement with:

- Magnetic shocks waves
  [Knudson *et al*., PRL **87** (2001) 225501]
- Spherical converging shock waves
  [Belov et al, Boriskov et al.]
- DFT results (e.g. Bonev et al.)

Recent measurements agree reasonably well with first principle methods but need to be verified.

V. Application to hot, dense helium

Helium DFT calculations agree well with gas gun shock experiment [Nellis PRL (1984)]

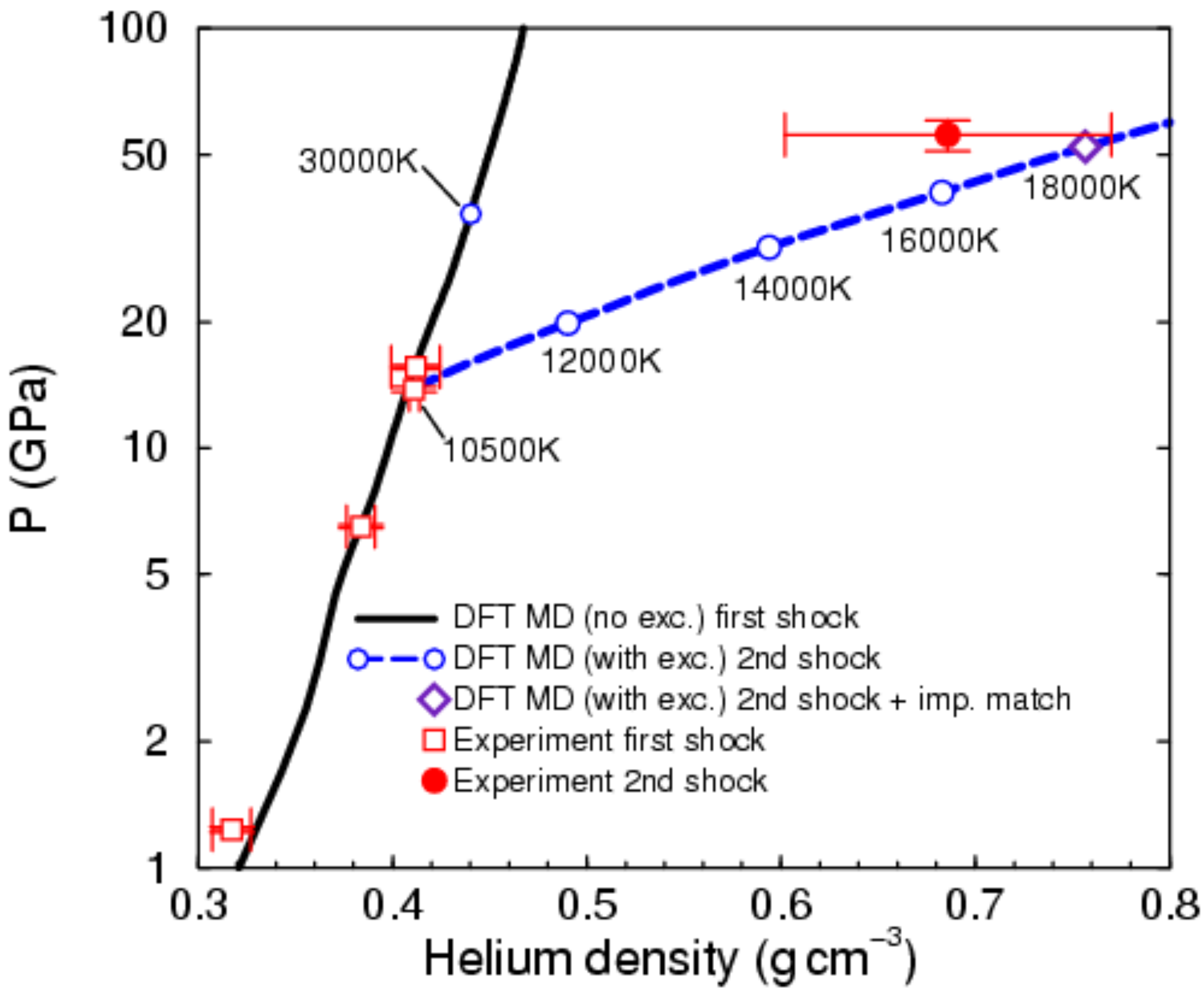

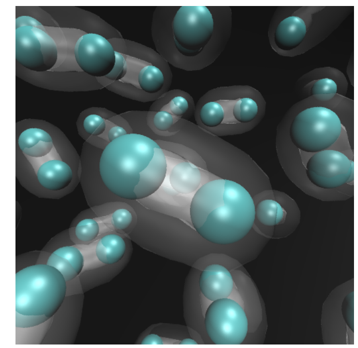

DFT-MD

DFT-MD and classical MC simulation yield less than 4-fold compression

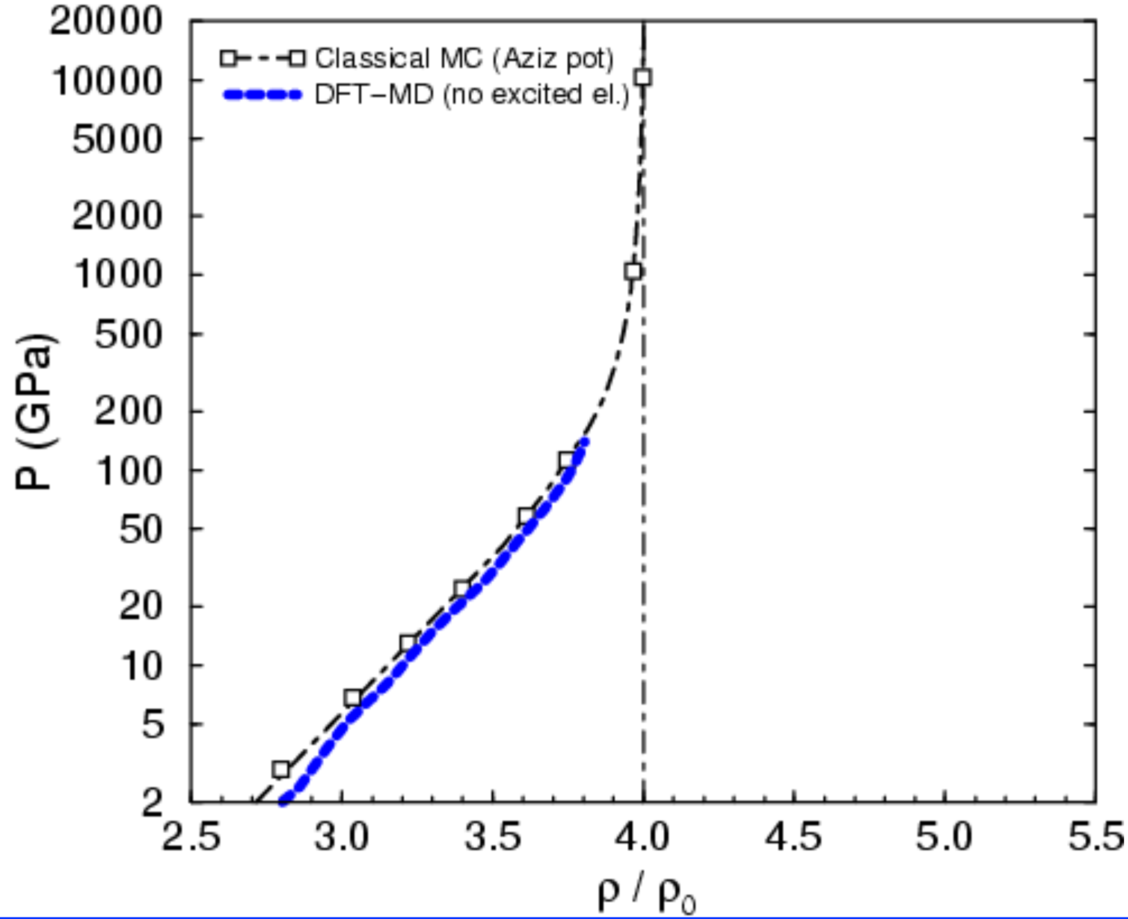

Classical MC simulation using the Aziz pair potential track the DFT-MD data reasonably well ⇒ compression less than 4-fold the initial density.

PIMC results yield more than 5-fold compression.

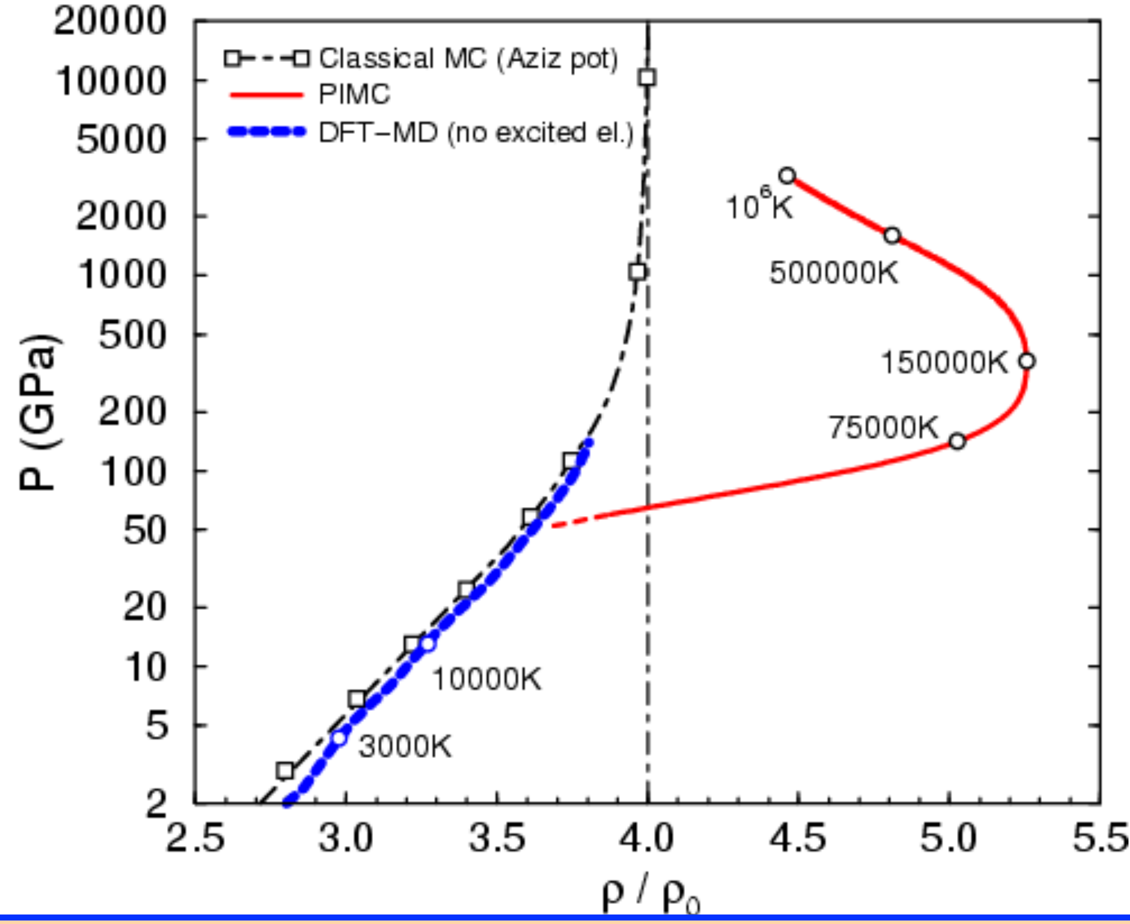

This high precompression is surprising because both PIMC and DFT-MD gave about 4-fold compression for hydrogen.

Add electronic excitations to DFT-EOS improves agreement with PIMC results.

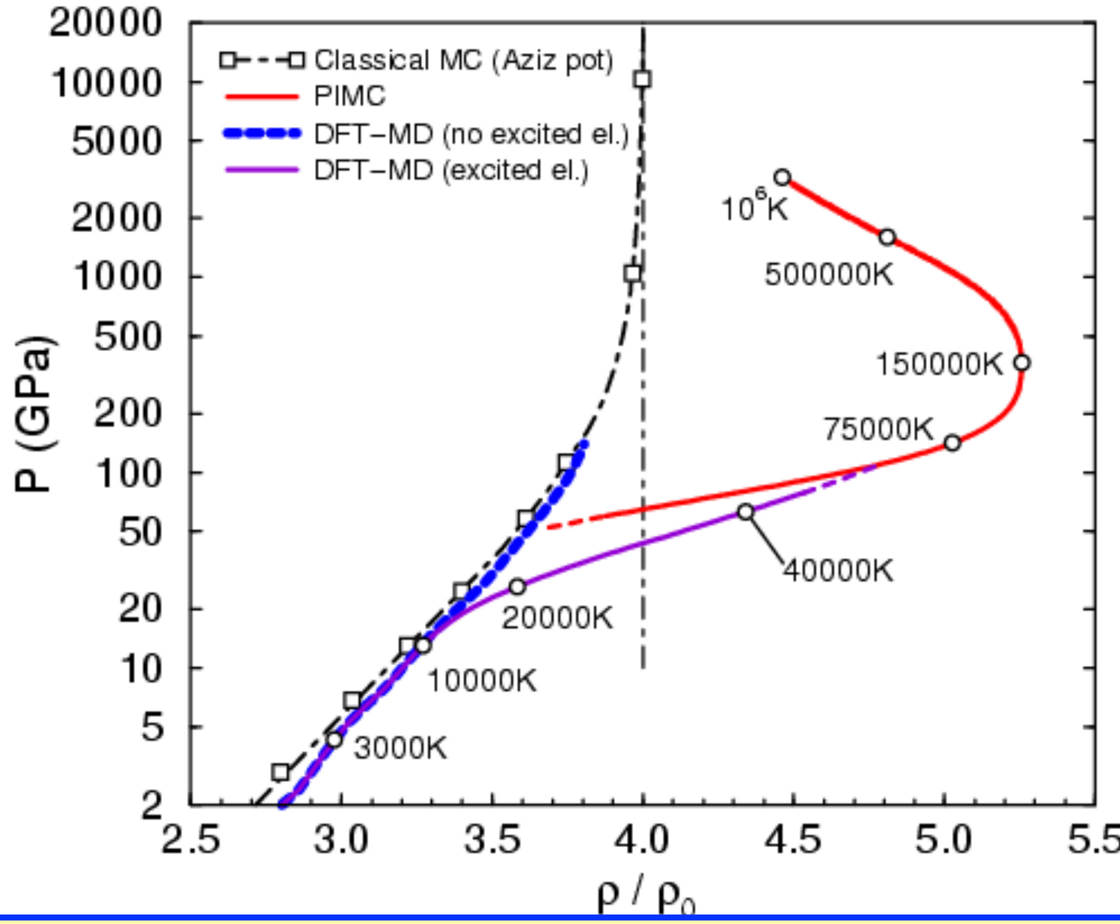

For a number of MD configurations, quasi-static finite-temperature electronic corrections to the EOS increase the compressibility.

Laser and Z-machine can probe regime of 5-fold compression

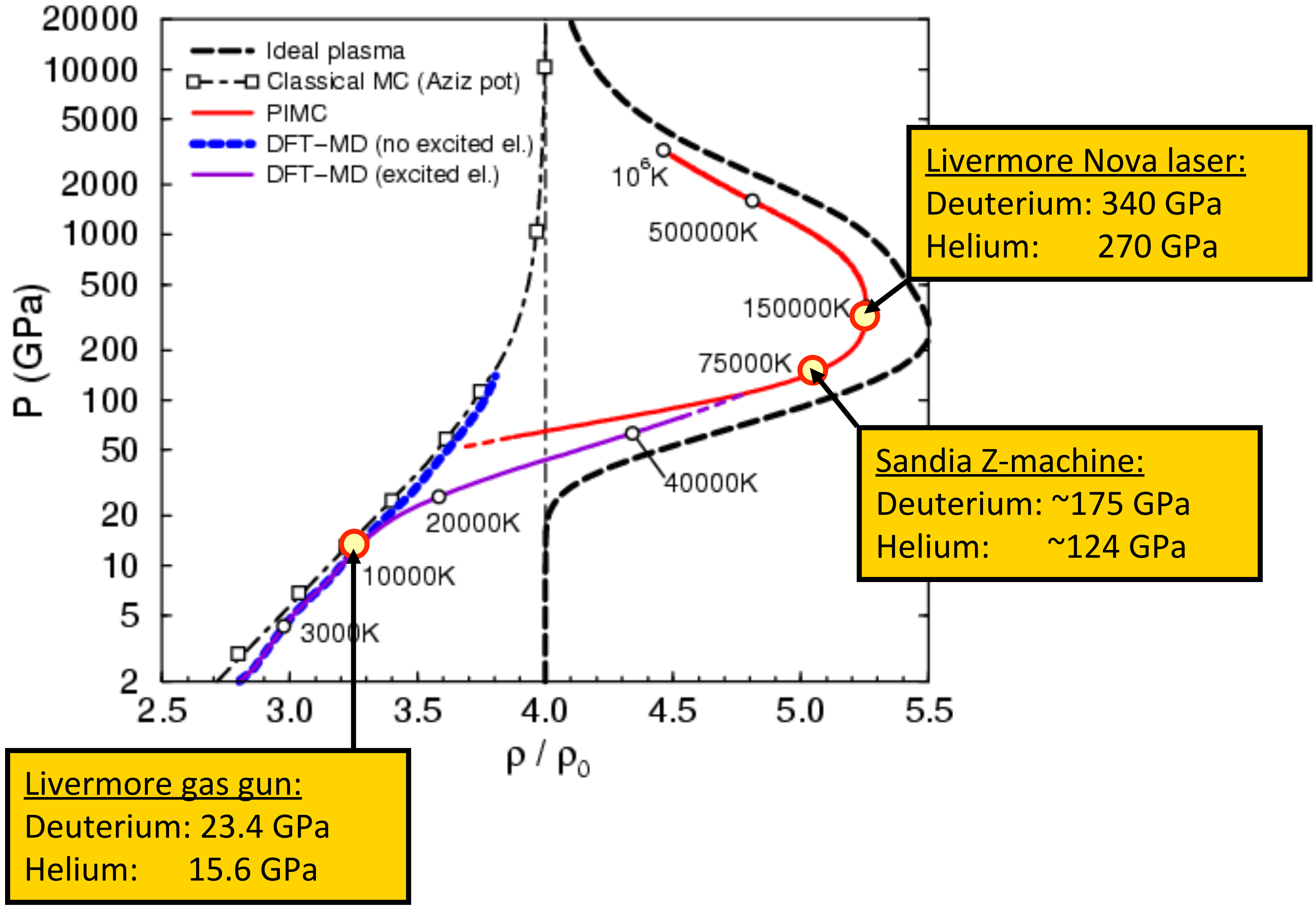

PIMC Calculations of the Helium EOS

Comparison with Saumon & Chabrier free energy model

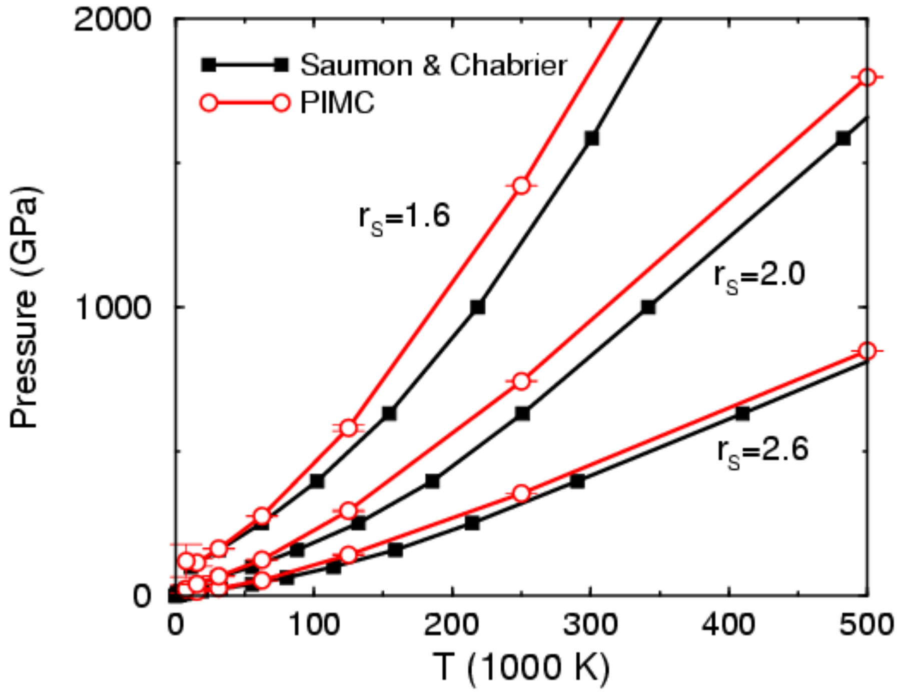

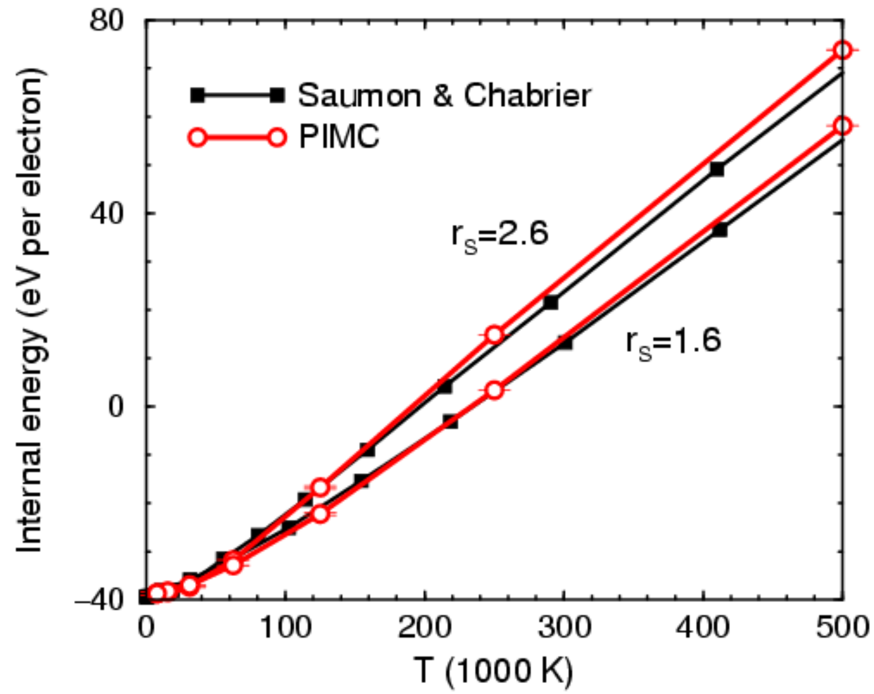

The pressure in severely underestimated by the SC model.

For Helium, PIMC and DFT-MD Simulations have been combined to make one consistent EOS table

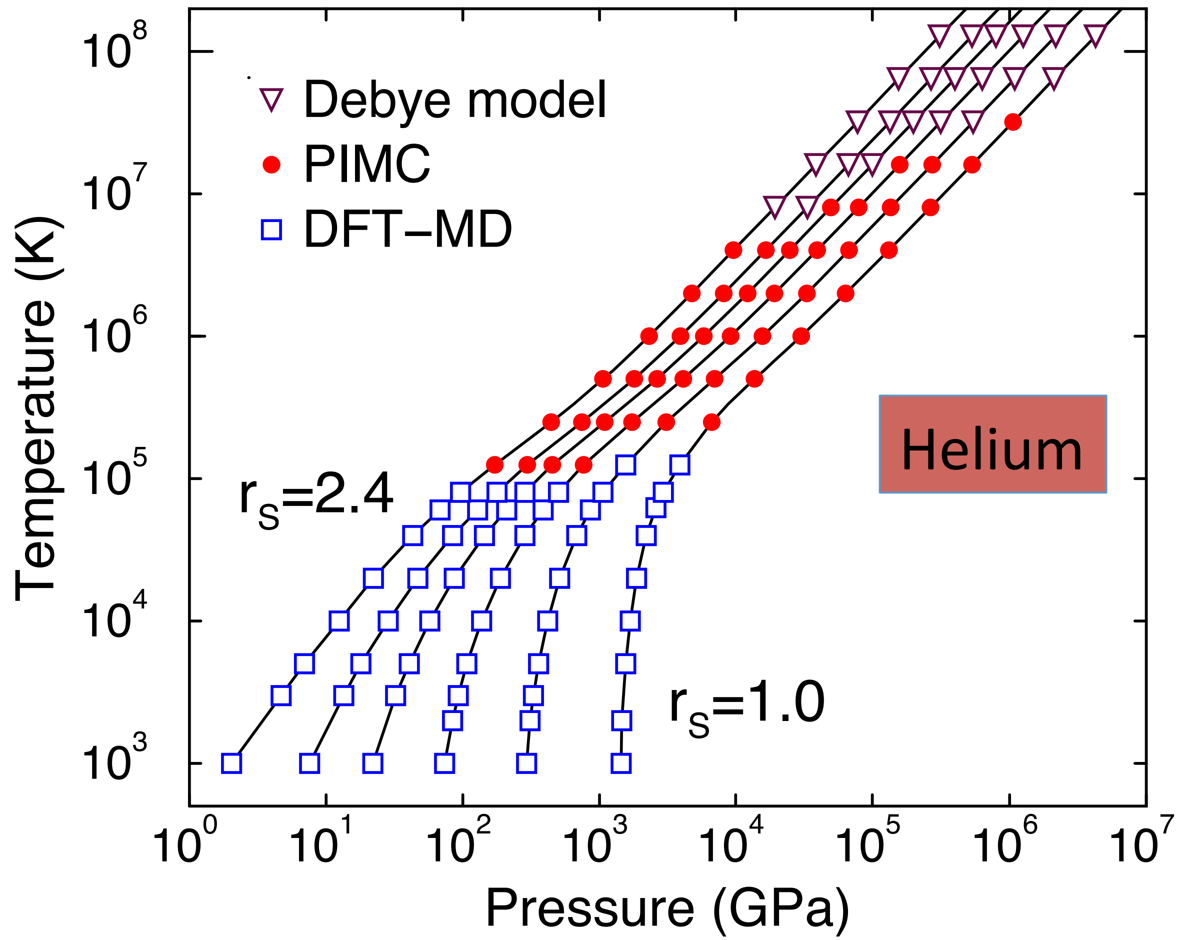

B. Militzer, *Phys. Rev.* B **79** (2009) 155105
B. Militzer, *Phys. Rev. Lett.* **97** (2006) 175501

For Helium, PIMC and DFT-MD Simulations have been combined to make one consistent EOS table

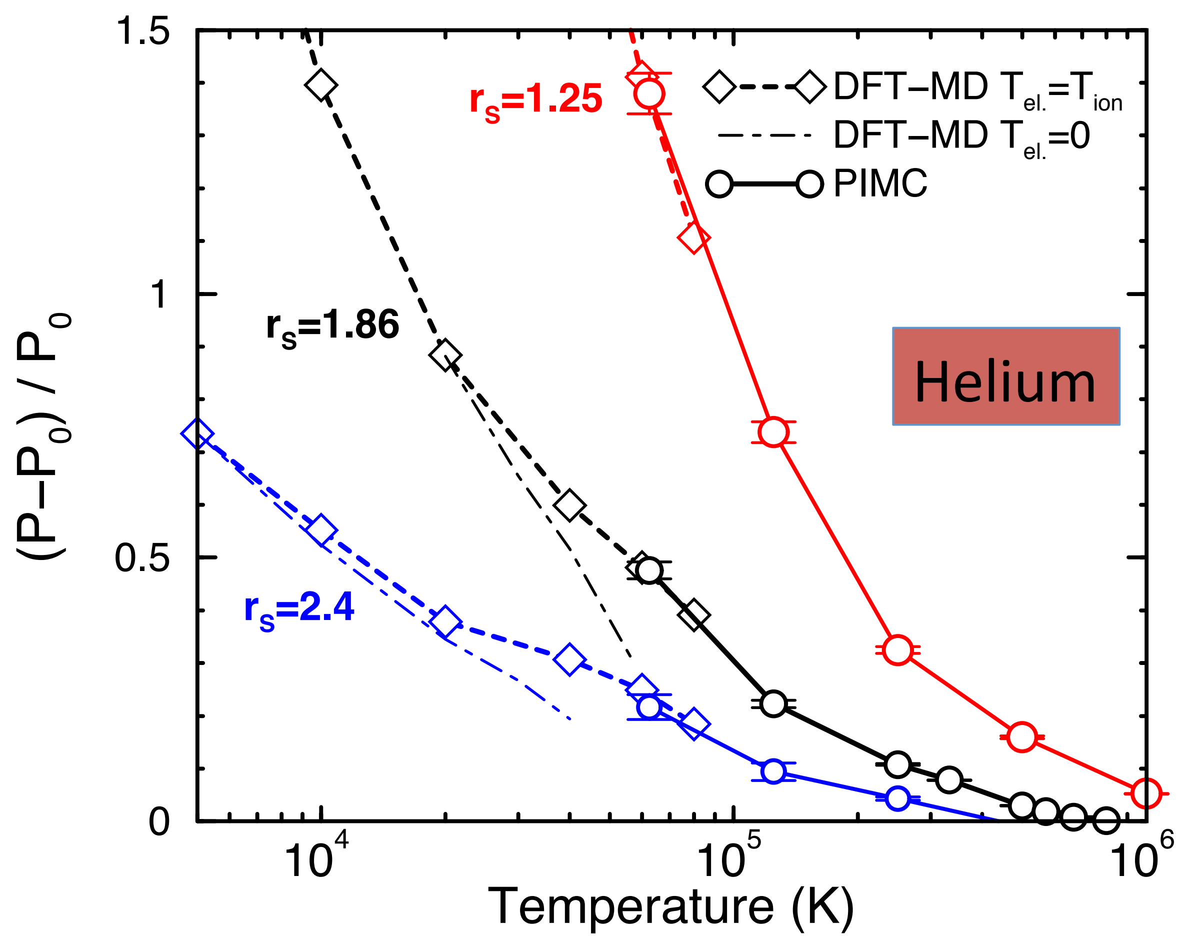

B. Militzer, *Phys. Rev.* B **79** (2009) 155105
B. Militzer, *Phys. Rev. Lett.* **97** (2006) 175501

New Experimental Technique: Combination of Static and Dynamic Compression

1) Static compression
Diamond anvil cell

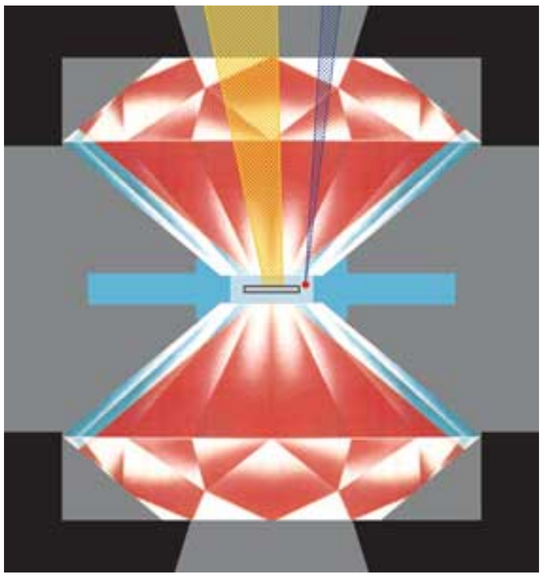

2) Dynamic shock comp.
Laser shocks

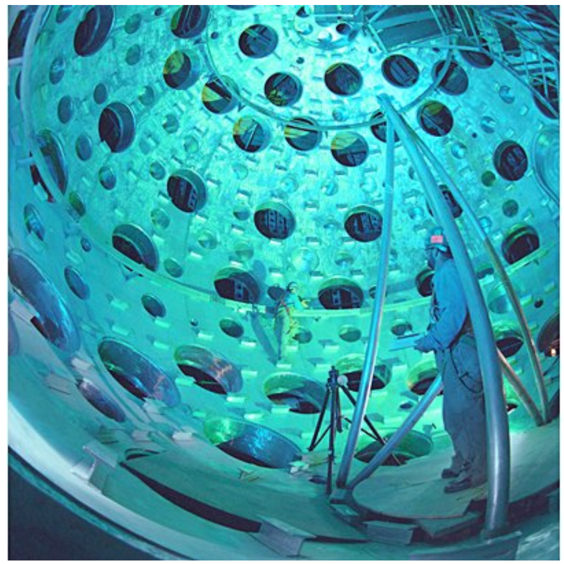

- LLNL-CEA collaboration
- Samples are **precompressed** in modified diamond anvil cell
- Precompression up to 1.5 GPa = 15 kbar

Comparison of PIMC Simulations with Laser Shock Experiments on Helium

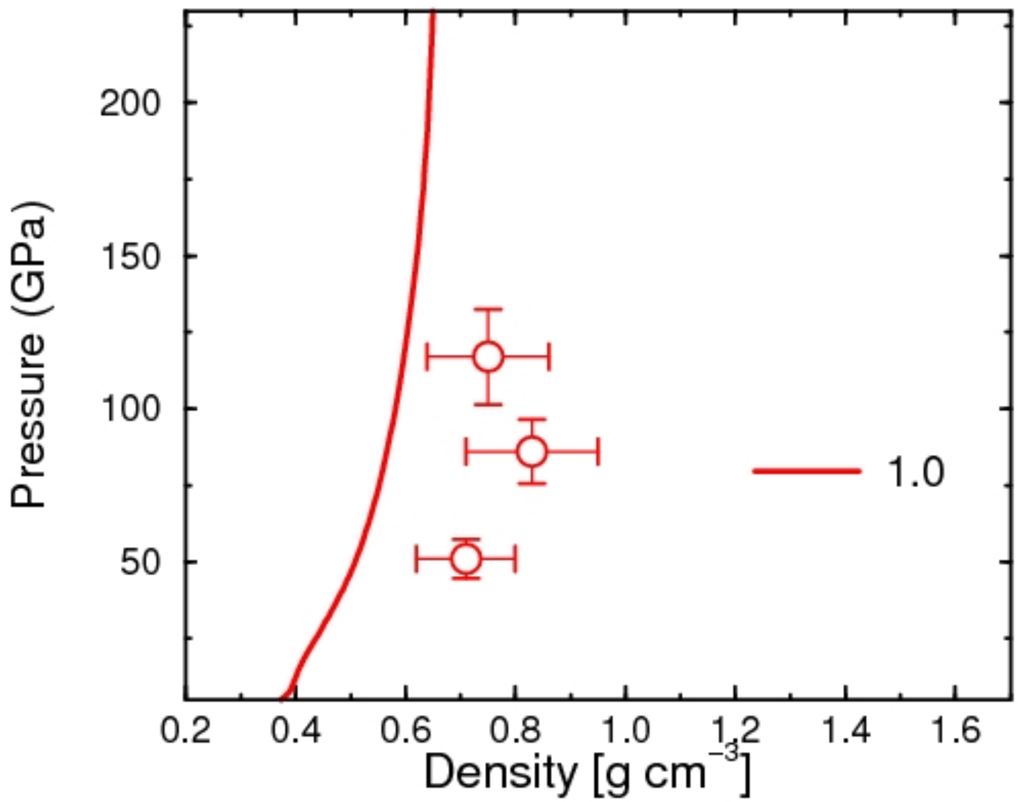

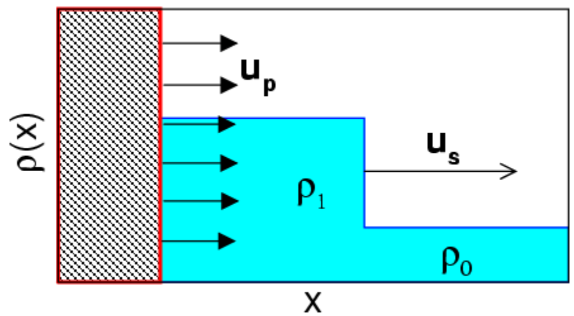

Diamond anvil cell

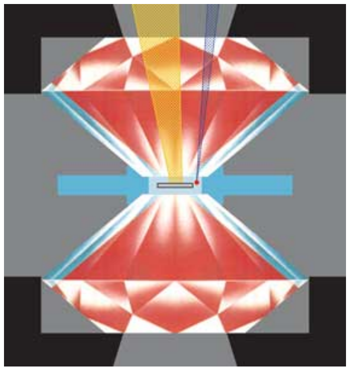

Laser shocks

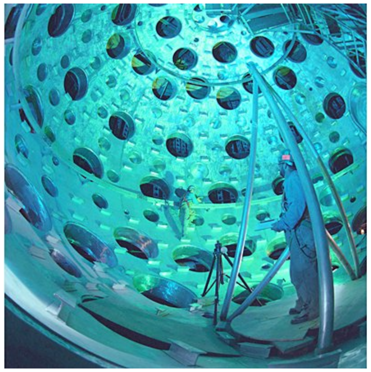

Theory: Militzer, *Physical Review Letters*, **97** (2006) 175501;

Exp: Eggert *et al. Physical Review Letters*, **100** (2008) 124503.

Comparison of PIMC Simulations with Laser Shock Experiments on Helium

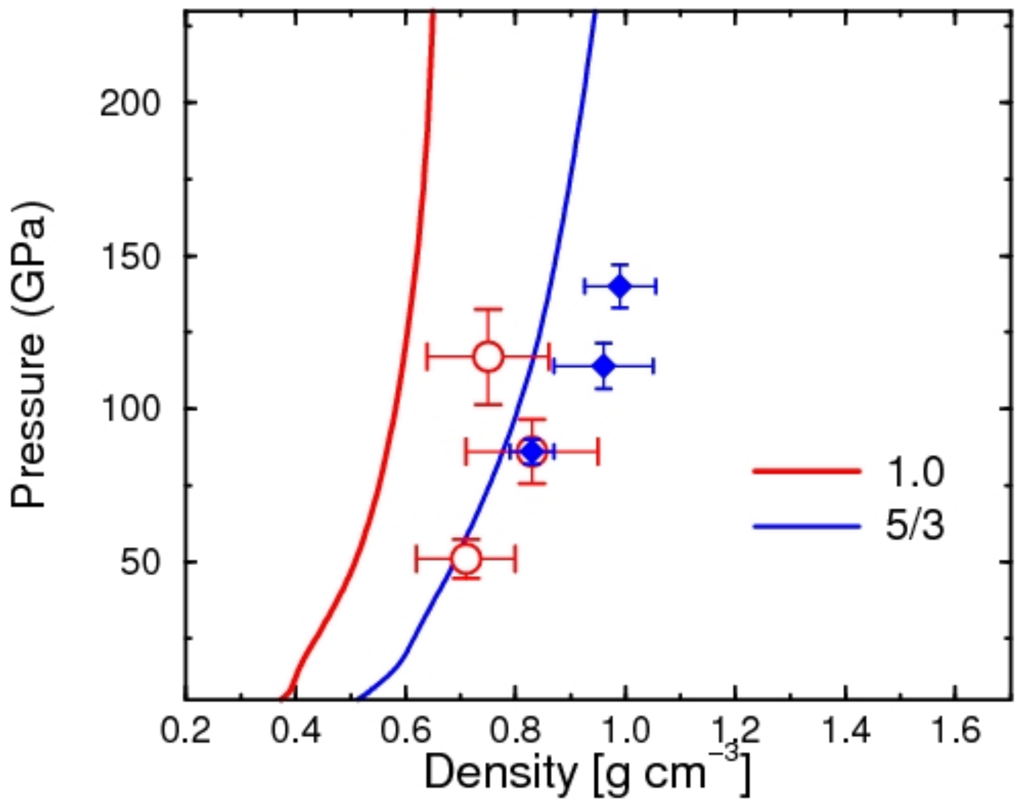

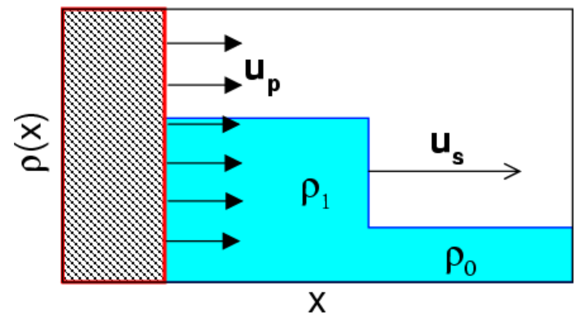

Diamond anvil cell

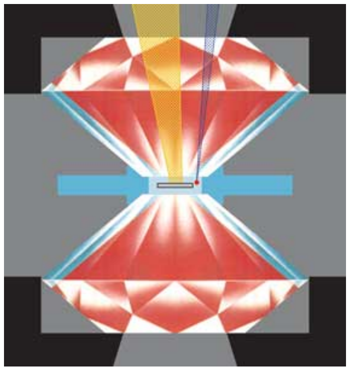

Laser shocks

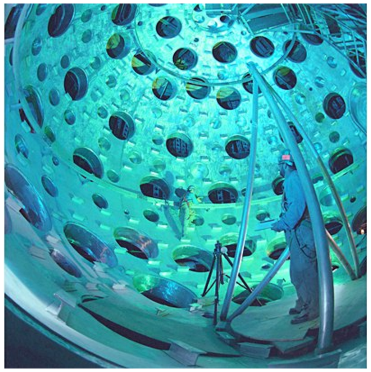

Theory: Militzer, *Physical Review Letters*, **97** (2006) 175501;
Exp: Eggert *et al. Physical Review Letters*, **100** (2008) 124503.

Comparison of PIMC Simulations with Laser Shock Experiments on Helium

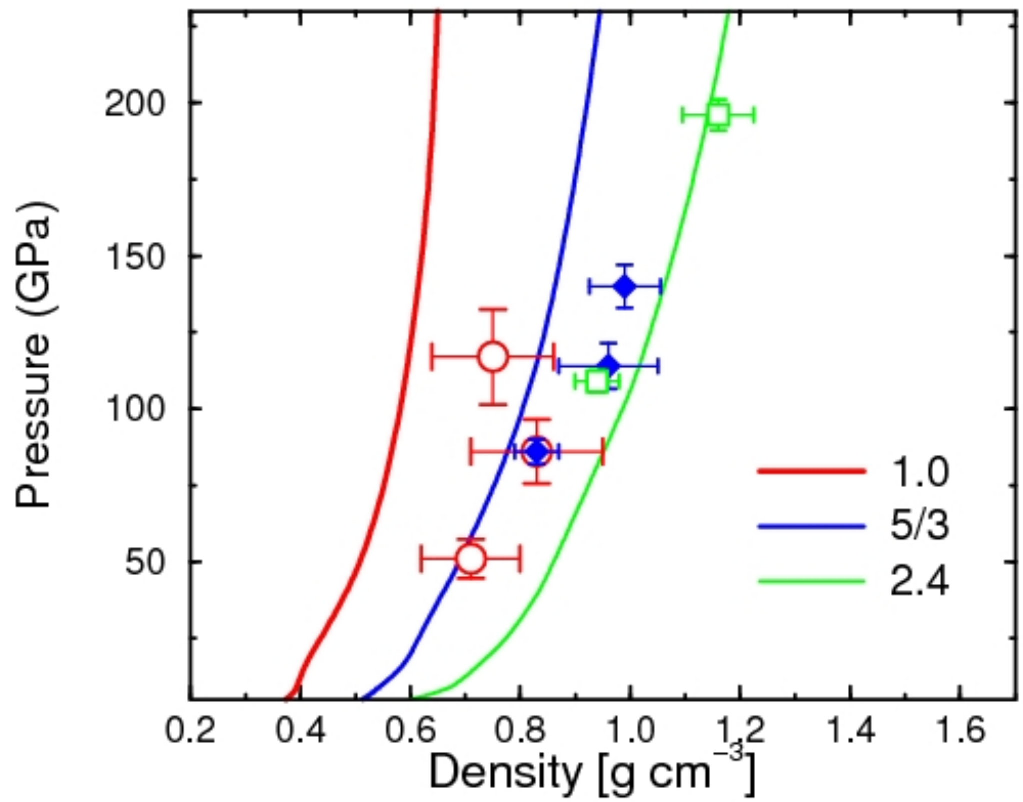

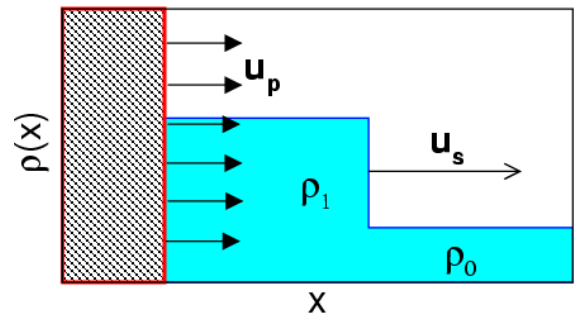

Diamond anvil cell

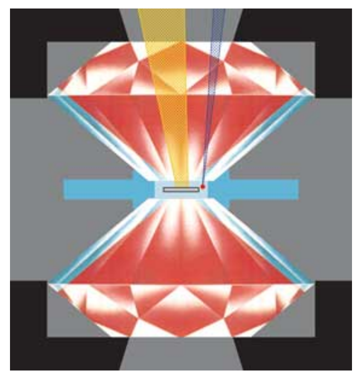

Laser shocks

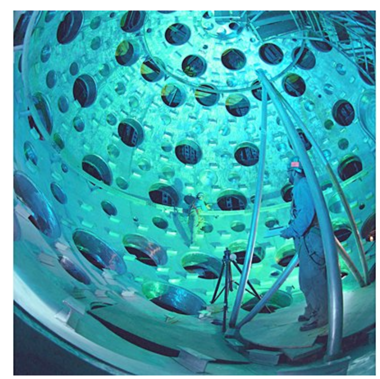

Theory: Militzer, *Physical Review Letters*, **97** (2006) 175501;

Exp: Eggert *et al. Physical Review Letters*, **100** (2008) 124503.

Comparison of PIMC Simulations with Laser Shock Experiments on Helium

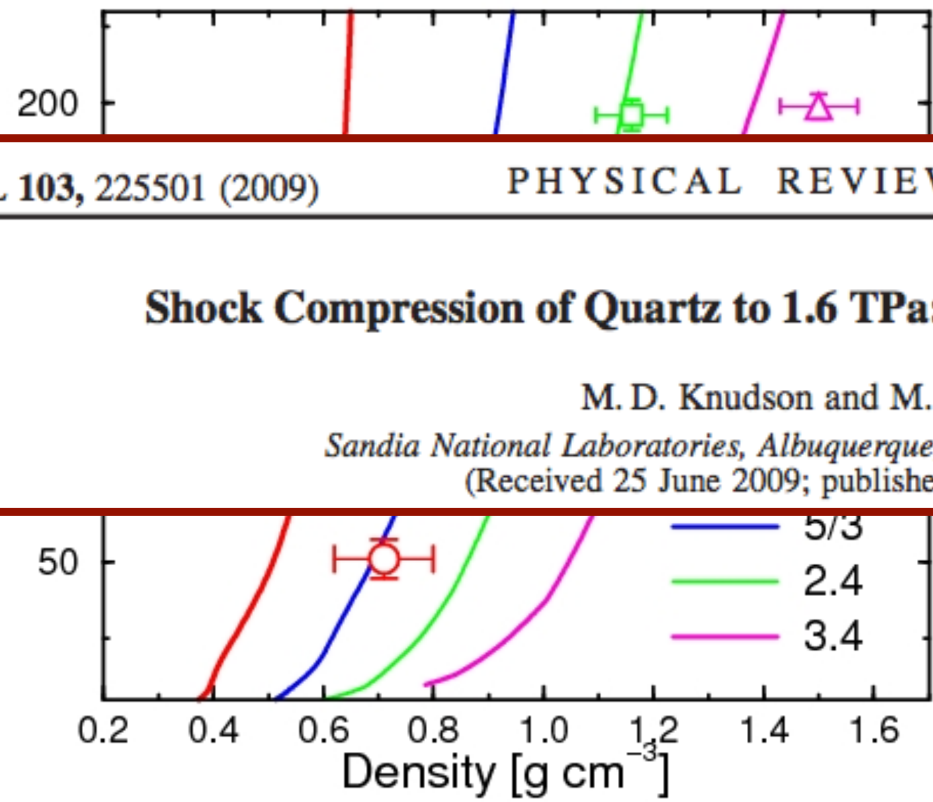

PRL **103,** 225501 (2009) PHYSICAL REVIEW LETTERS week ending 27 NOVEMBER 2009

Shock Compression of Quartz to 1.6 TPa: Redefining a Pressure Standard

M. D. Knudson and M. P. Desjarlais
Sandia National Laboratories, Albuquerque, New Mexico 87185-1195, USA
(Received 25 June 2009; published 24 November 2009)

Principal Hugoniot:

PIMC and experiment agree.

Theory: Militzer, *Physical Review Letters,* **97** (2006) 175501;
Exp: Eggert *et al. Physical Review Letters*, 100 (2008) 124503.

VI. PIMC of Carbon and Water Plasmas

Regime of Warm Dense Matter requires new simulation techniques – Application ICF experiments

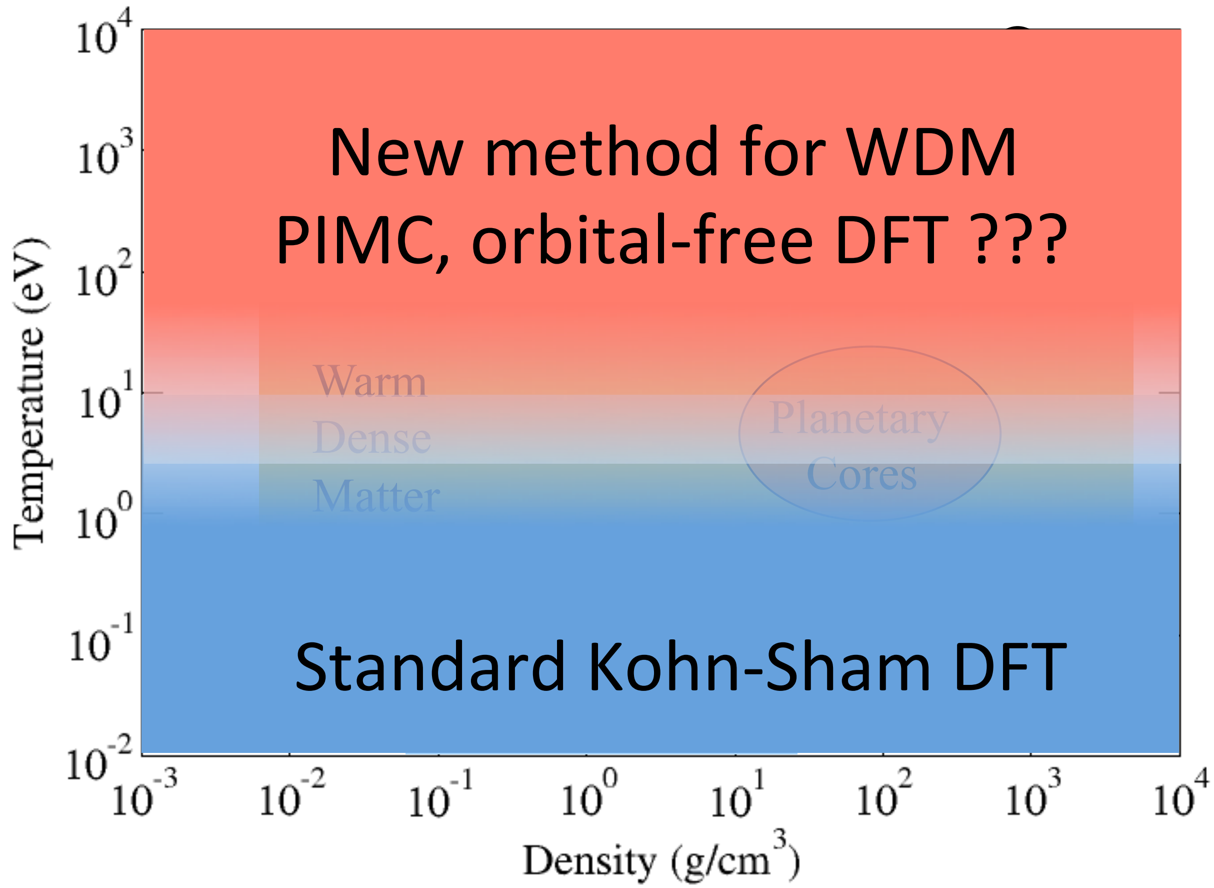

ICF Hohlraum

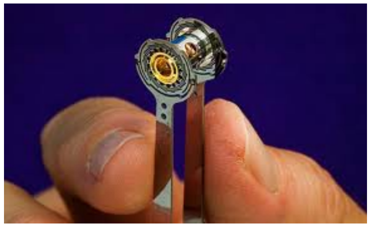

ICF Capsule

Effects of bonding, ionization, exchange and correlation, and quantum degeneracy all important.
Carbon is a promising ablator for Inertial confinement fusion (ICF).
We are working with LLNL on carbon EOS.

Why were there no PIMC calculations for elements heavier than helium until 2012?

Problem 1: **Nonlocal pseudopotentials** in fermionic path integrals

$$\langle R \,|\, \hat{\rho}_{n.l.} \,|\, R' \rangle = \langle R \,|\, e^{-\tau[\hat{T}+\hat{V}_{n.l.}]} \,|\, R' \rangle$$

$\rightarrow$ Sign problem even for the 1-particle scattering problem.

Problem 2: **More accurate nodes** needed at low temperature.

Problem 3: Acceptance ratio of **reference point moves** decreases at low temperature. Low sampling efficiency.
Hydrogen: $T > 0.1 \times T_{fermi}$

Alternative: Coupled Electron-Ion Monte Carlo (Delaney, Pierleonie, Ceperley)

Reintroduce Born-Oppenheimer approximation:

Classical MC for the ions ($T_{ion} > 0$)

QMC for the electrons ($T_{el} = 0$)

First Path Integral Monte Carlo Simulations for Heavier Elements Fill this Gap in Temperature

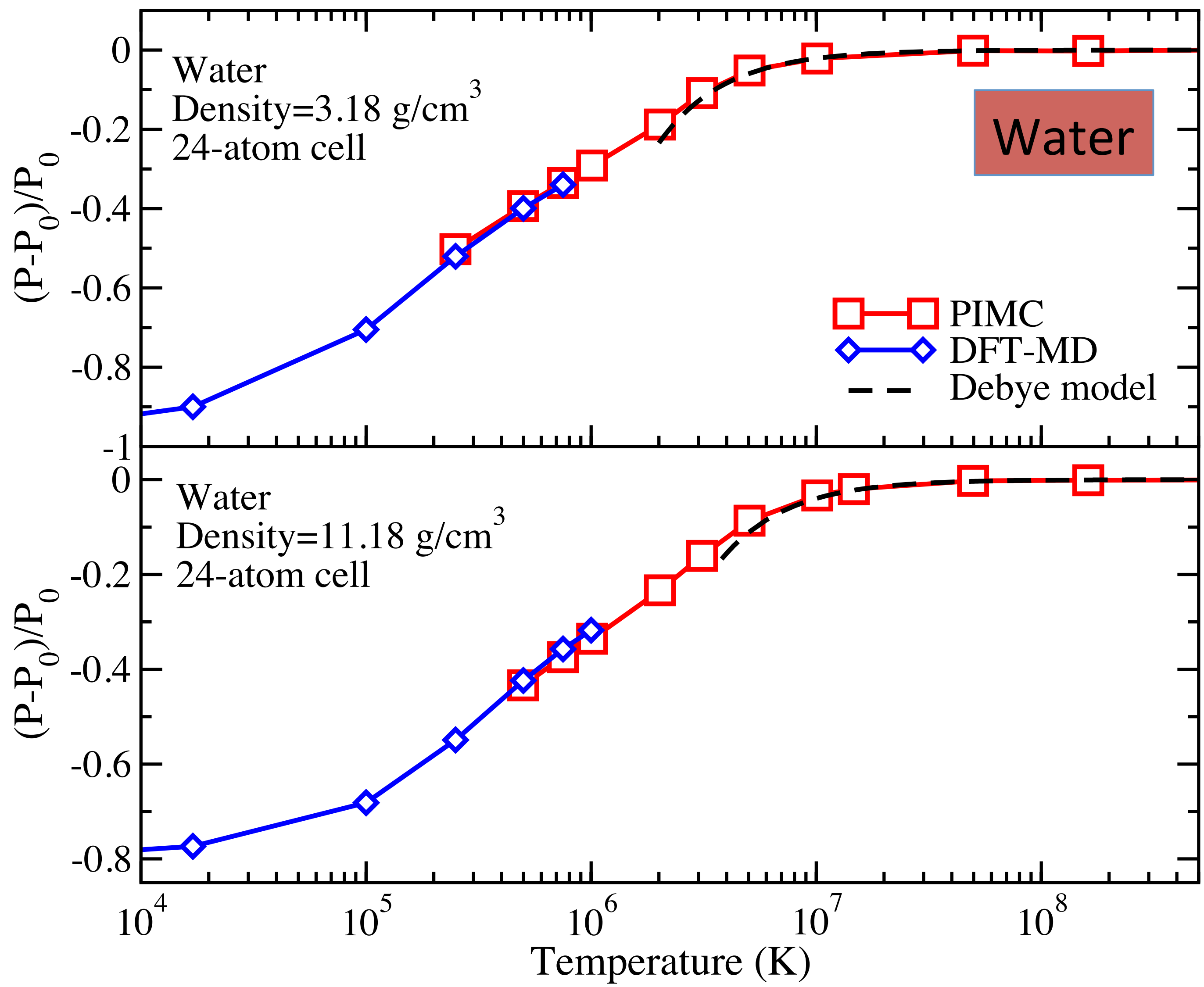

Again Path Integral Monte Carlo bridges the Gap in T between DFT-MD and the Debye Model

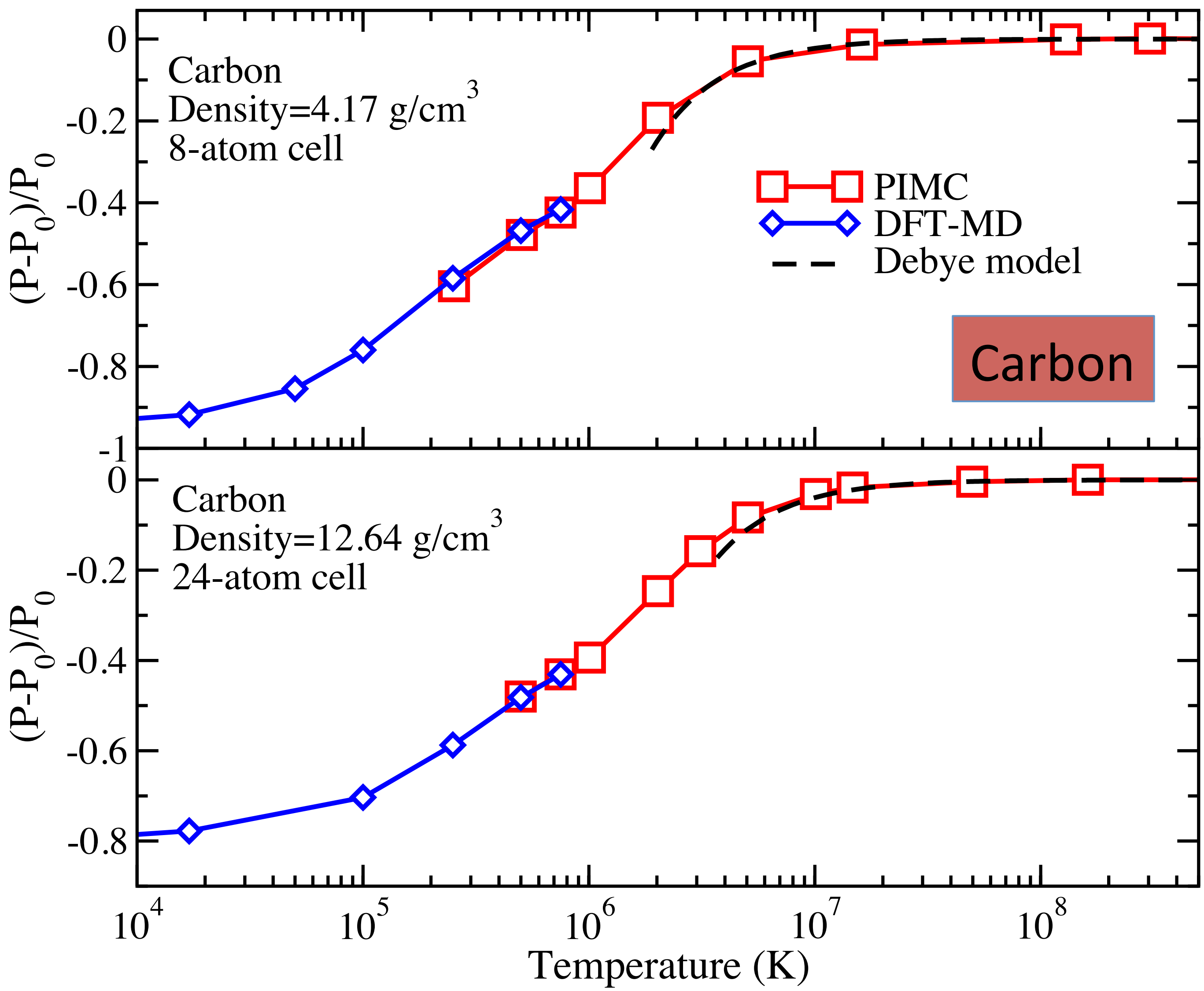

Path Integral Monte Carlo bridges the Gap in Internal Energy vs Temperature for Water and Carbon Plasmas

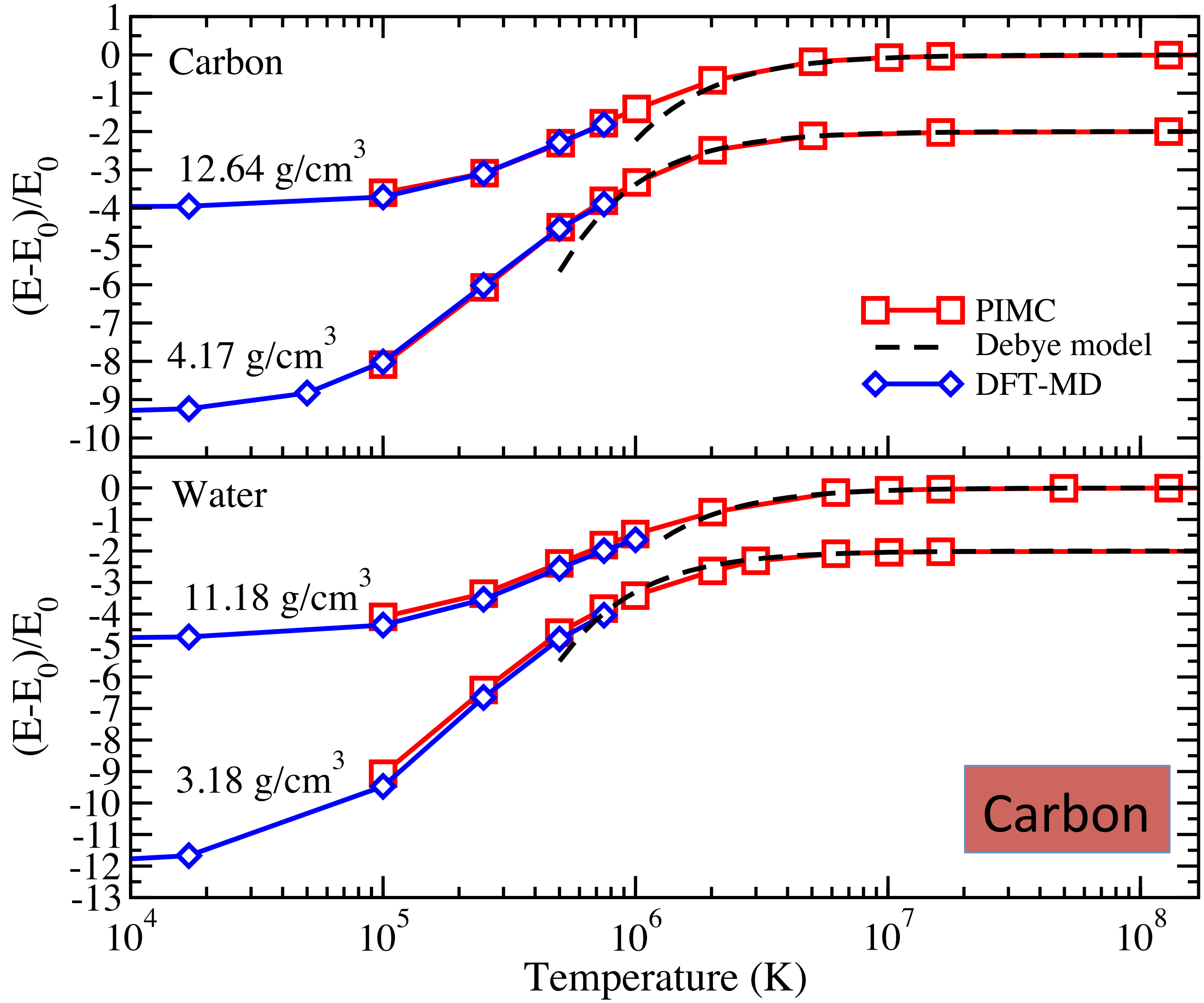

Carbon

Study Structural Properties: Pair Correlation Functions for Water and Carbon Plasmas

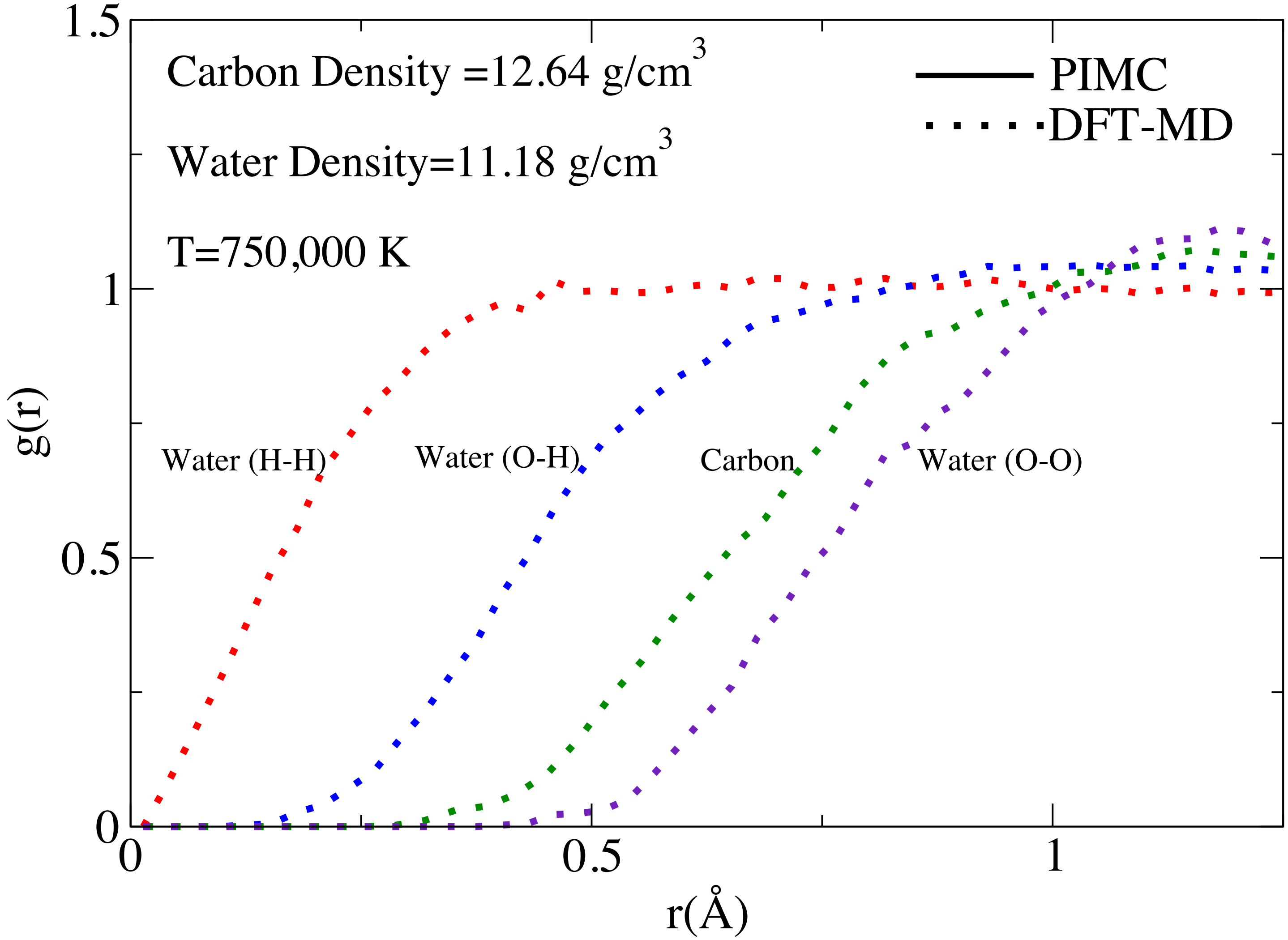

Path Integral Monte Carlo and DFT-MD are in very good agreement

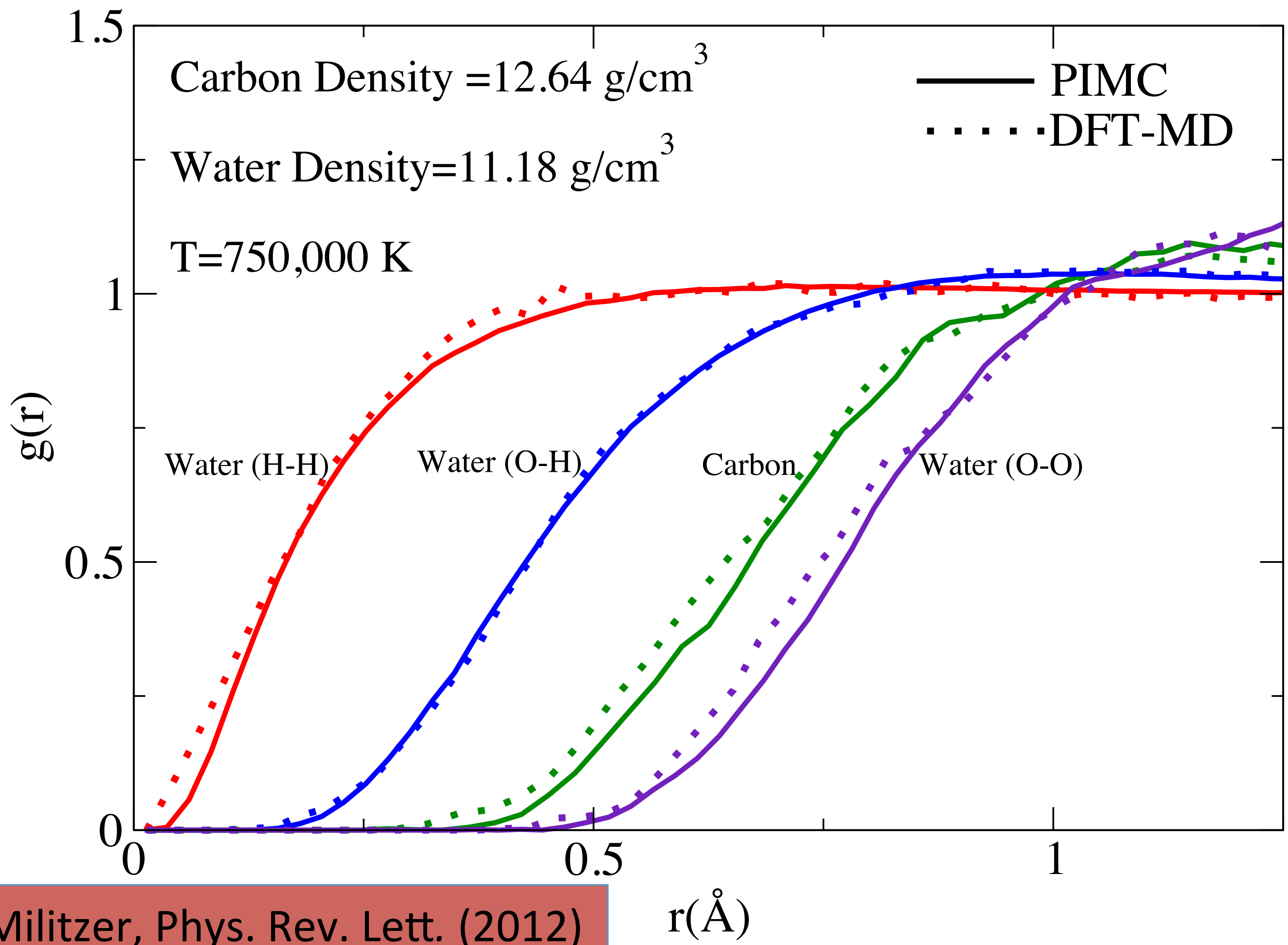

Driver, Militzer, Phys. Rev. Lett. (2012)

Why do free-particle nodes work for PIMC simulations of first-row elements?

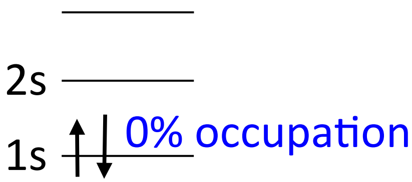

Core electrons are **fully ionized.**
Free-particles nodes are **ideal!**

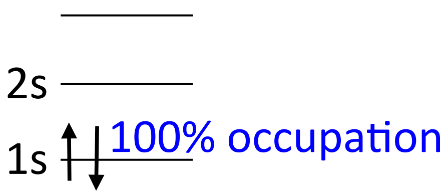

1s state doubly occupied. Others ionized.
Free-particles nodes should still work.

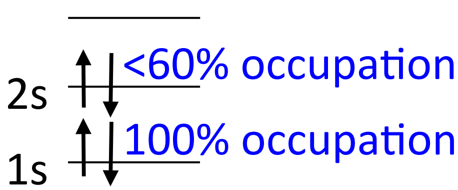

1s 100% occupied, **2s less than 60% occupied**
Free-particles nodes in PIMC are accurate for T > 250,000 K for carbon and water plasmas.

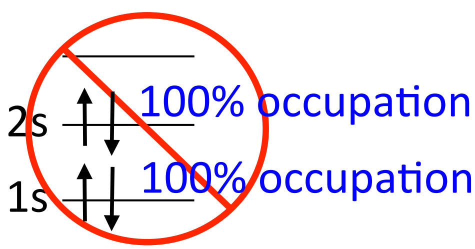

2s 100% occupied. Free-particles nodes do no longer work **but KS-DFT works!**

Summary

- Presented new path integral Monte Carlo simulations for heavier elements (all-electron simulations, free particles nodes).
- Very good agreement with DFT for carbon and water plasmas.
- No insufficiencies in the ground-state exchange-correlation functionals.
- We constructed again consistent EOS table for C and H_2O.
- More materials to be studied. Please make suggestions!

Driver, Militzer, Phys. Rev. Lett., 108 (2012) 115502.

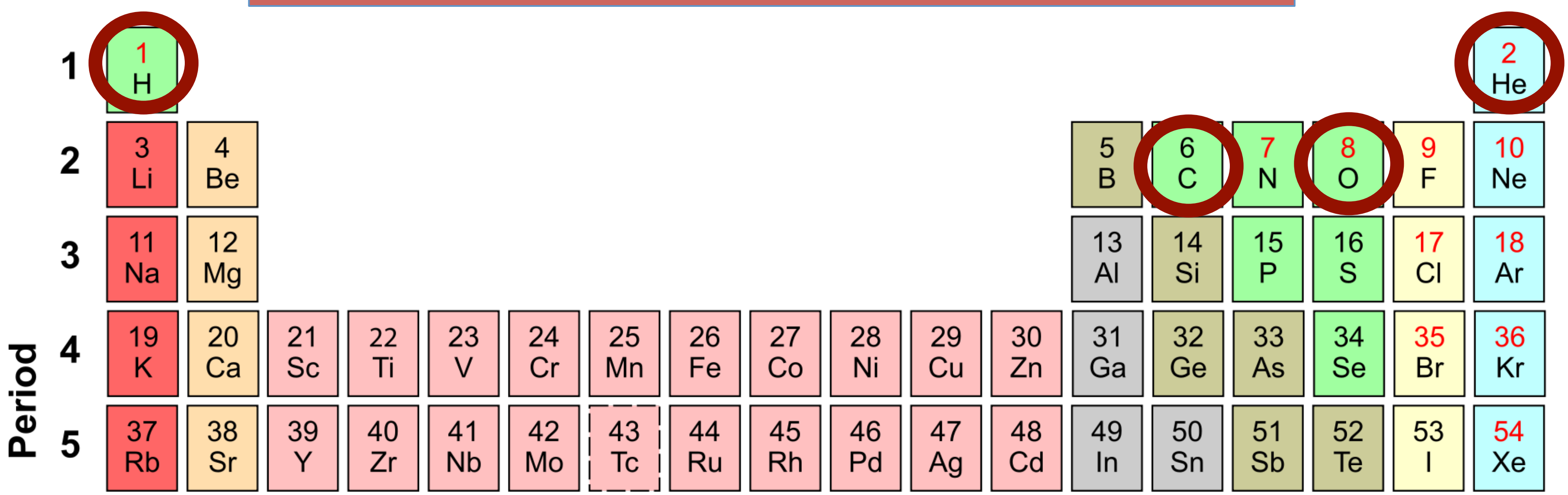

The End